2006:221 CIV

MASTER'S THESIS

MELTING

Pre-study of models and mapping
Physical modeling of scrap melting

MARIANNE ÖSTMAN

MASTER OF SCIENCE PROGRAMME
Engineering Physics

Luleå University of Technology
Department of Applied Physics and Mechanical Engineering
Division of Physics

2006:221 CIV • ISSN: 1402 - 1617 • ISRN: LTU - EX - - 06/221 - - SE

Foreword

This master thesis has been very interesting to work with. The pre-study contained works in several different areas of both mathematics and physics. I have learnt more about different processes in steel manufacturing. This has been 20 weeks of intensive learning and development and I have learnt a lot about melting processes.

I like to thank the personnel of Mefos – Metallurgical Research Institute AB, in Luleå especially my supervisor Jonas Alexis. A special thank for help, with the construction of the physical model Seymour Eriksson, Anders Strålberg and Kjell Öström. I also would like to thank my supervisor Niklas Lehto at Luleå University of Technology for the discussions and comments during the preparation of the manuscript.

Abstracts

A lot can be won by better use of the steel. For example the higher strength the less material is needed and less material gives easier transportation, less discharge and energy and need less resource. Scrap has been used in steel industry for over a century.

This master thesis is a part of a European commission project called “Control and optimisation of scrap charging strategies and melting operations to increase steel recycling ratio”. Mefos is a partner of that project and this master thesis contains the parts “Pre-study of models and mapping” and “Physical modelling of scrap melting”.

Melting of scrap metal is of increasing interest to the metallurgical industry since it allows the recycling of metals at a fraction of the original production cost. This is in some way a new area, which is seen by the results in the study. But in some areas this has been looked on, for example in Japan and Canada there has been some interesting work on this field. Some theories of melting are commented, and examples are given on the enthalpy-porosity method, the conservation element/solution element method and the homogenization theory.

This master thesis is presenting melting of scrap steel in an EAF, electric arc furnace. The melting process is depending on the heat transfer from the arc and the convective heat transfer in the liquid metal. Scrap metal refers to either metal chopped from the end of ingots or compressed blocks of used beverage containers. This means that the scrap is of various shapes. The heat and mass transfer between liquid and solid phases results in a complex problem. As soon as the melting begins the molten liquid drips down toward the bottom of the furnace. Thereafter, the molten liquid level rises while the height of the scrap metal decreases. The scrap is heated both from the arc and the molten liquid at the bottom.

In the physical model the electric arc is simulated by a hot-air gun, melting ice instead of iron scrap. The experiments in the physical model are to be used as input in a CFD-analysis. CFD stands for Computational Fluid Dynamics, and is a form of computer simulation.

Contents

FOREWORD **1**

ABSTRACTS **1**

CONTENTS **1**

1 INTRODUCTION. **3**

2 STEEL AND SWEDISH STEEL INDUSTRY **4**

2.1 THE PROCESS OF MAKING STEEL 4
2.2 CHARACTERISTIC'S OF STEEL 6

3 STEEL AND THE ENVIRONMENT **8**

3.1 ENERGY AND POWER 8
3.2 ENERGY CONSUMPTION IN THE STEEL MAKING PROCESS 9
3.3 REST-PRODUCTS 11

4 SCRAP **12**

5 ELECTRIC ARC FURNACES (EAF) **14**

5.1 DIRECT-ARC ELECTRIC-FURNACES 15
5.2. CHARGING SCRAP 19
5.3. VOLTAGE AND POWER 20
6.1 CONDUCTION 24
6.2 CONVECTION 25
6.3 RADIATION 25
6.4 MELTING IN A MELTING FURNACE 26

7 MATHEMATICAL MODEL OF MELTING **28**

7.1 ENTHALPY-POROSITY METHOD 28
7.1.1 Heating stage *29*
7.1.2 Enthalpy method *31*
7.1.3 Numerical Schemes *33*
7.2 THE CE/SE METHOD 35
7.2.1 Governing equation, enthalpy method *36*
7.2.2 Numerical method: CE/SE *38*
7.3 HOMOGENIZATION 48

8 THE PHYSICAL MODEL **53**

8.1 BUILDING THE MODEL 54
8.2 RESULTS AND DISCUSSION 58
8.2.1 Air flow *58*
8.2.2 Melting time comparison *60*
8.2.3 Differences between the EAF and the water/ice model *62*
8.2.4 Comparison results *64*

9 FUTURE DEVELOPMENTS AND CONCLUSIONS **66**

10 REFERENCES **67**

APPENDIX **70**

APPENDIX 1 70
Classification of steel scrap *70*
APPENDIX 2 72

Contents

Nomenclature *72*
APPENDIX 3 73
Photos of the measurement equipment *73*
APPENDIX 4 76
Tridiagonal matrix algorithm (TDMA) *76*
Fourier Biot *76*
Divengence Theorem *77*
Delaunay triangulation *78*
Taylor series *79*
Weighted mean *79*
Permutation *80*
Weak formulation *80*
R^2 ..... *80*

1 Introduction.

Melting of scrap metal is of increasing interest to the metallurgical industry since it allows the recycling of metals at a fraction of the original production cost. The knowledge about optimum melting conditions of various scrap grades is mostly limited to conclusions drawn from statistical analyses of industrial operations with complex scrap mixes. It is likely that the optimisation of operating practices as a function of the scrap mix used is highly significant with regard to furnace efficiency but is not fully achieved in most EAF (Electric arc furnace) plants. Studies of melting may streamline the scrap melting procedure.

Studies of melting are in some way a new area for the steel industry, which can be seen from the results in this study. But in some areas this has been locked on, for example in Japan, Australia and Canada there has been some interesting work on this field, [1-6]. The melting in other areas than in the steel manufacturing is therefore of great interest.

This work starts with an investigation of what so far has been written on the subject of melting modeling in an EAF. The next step is to figure out how to construct the model and order material. Experiments are performed on the finished model. The evaluation of the test results are meant to be used as input to a numerical model of melting, which is not included in this master thesis.

The melting of steel in an electric arc furnace is a complex problem, consisting of heat and fluid flow, mass transfer and electromagnetic phenomena. In general, the numerical simulations used for phase change problem are classified into two different approaches: the fixed-grid or the transformed-grid methods.

Some mathematical models are presented in chapter 7. Enthalpy-porosity method is often used in numerical melting simulations, and is a fixed-grid method combined with a porous media [2, 4-7]. The method of space time conservation element and solution element is developed to solve conservation laws. It is especially made for physical problems with a region that is difficult to realize numerically, such as boundary layer in melting, [7-10]. The homogenization theory is an analytical method of solving partial differential equation, which can be used on porous media and composites. It is often used together with numerical simulations [11].

2 Steel and Swedish Steel industry

Steel is the most important industrial material, used in building, cars, computers, different machinery, tools, household utensils, etc. To take care of the numerous variations of use of the steel a similar variation in steel quality is needed. Steel is a group of several different kinds of materials, all made of iron and all suitable for recycling and reuse.

The Swedish steel industry is very competitive. The productivity has almost doubled during the last decade. The Swedish steelworks deliveries of commercial finished steel products (*i.e.* sheet metal, "band", wire, bar, profiles and pipes) totalled 5.2 million tons to the value 47.5 milliard SEK, 2004. About 85 % of the deliveries were exported. About three quarters of the commercial finished steel were further refined by the manufacturing industry to finished products. Most of the remaining part goes to the building industry. Rails and reinforcement steel are examples of "commercial steel" that are finished products directly after manufacturing in the steelwork [12].

Swedish steel companies commit far more on research and development than other steel companies around the world. They stake about one milliard SEK per year on steel research, which is equivalent to 2 % of the total Swedish steel industry's turnover [12]. Swedish steel industry has, as the steel industry in the rest of the world gone through major changes in the structure. The Swedish steel companies are specialised in their own area where they have developed advanced steel qualities and steel products. This has resulted in less competition between the companies in Sweden. Today, many of the Swedish steel companies are world leading in their particular area [12].

2.1 The process of making steel

Today metallurgical processes are controlled by advanced information technology. The basic condition to be able to produce steel of high quality efficiently is a good control of the raw materials. The two most important raw materials in steelmaking are iron ore and scrap.

Bought scrap, together with scrap from the own production are charged in an electric arc furnace. The vault on the furnace is put in place and the scrap melts. The hot exhaust from the arc furnace is often used to preheat scrap to the furnace. The liquid steel from the arc furnace is drawn into a container, a so called ladle, which will be transported to a ladle-station. Here the composition and temperature of the steel can be adjusted before casting. When stainless steel is produced a converter is used instead of a ladle to give the steel the right composition and temperature before casting. The liquid steel is cast in a continuous casting machine. Steel that will go to the rolling-mill inside the work has to be heated to rolling temperature, 1200 ^{o}C. This heating is made in a furnace that can be

heated by electricity or fuel (LPG[1], oil, gas from the coke furnace) [12]. See Figure 1. Before delivery the steel can be treated in various ways after the customer's wishes.

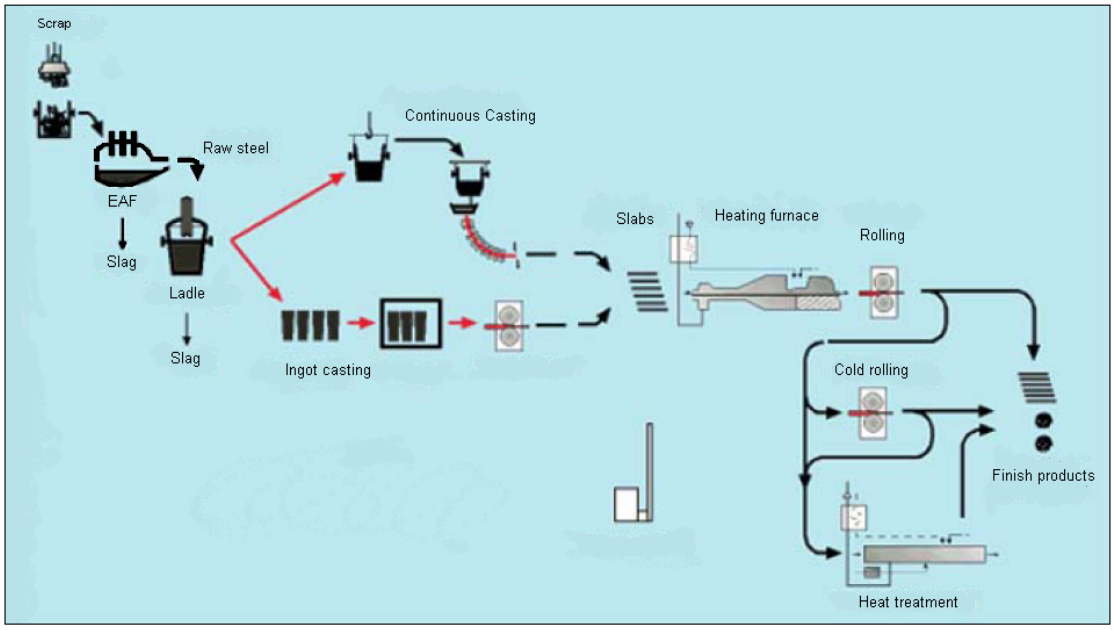

Figure 1. Overview picture of the steelmaking process from scrap to finish product.

In scrap based steel manufacturing, electric arc furnaces are mainly used for melting. In Sweden scrap-based steel is produced at eleven locations, which together produces 2 million tones. The whole world produced 356 million tons of scrap based steel in 2004 [12].

Steel can also be obtained from iron ore, which has to be enriched before use. The iron ore is reduced to iron by removing oxygen from the oxidant iron minerals with coke in the blast furnace. The raw iron from the blast furnace contains iron and also 3-4 % carbon and other substances. In Sweden there are blast furnaces in Luleå and Oxelösund, which together produces more than 3.9 million tons raw iron, of the world production of about 718 million tons (2004). The world production of ore-based raw steel was 662 million tons in 2004 [12].

The raw iron usually goes to the steel work in liquid form. In ore based steel production steel is produced mainly by raw iron, but about 20 % steel scrap is added. The carbon content is reduced with oxygen in a converter. The reaction of the oxygen and carbon gives heat, by burning the exhaust. Products that are not gases assemble in a slag. The quality of the steel is controlled by using different substances to produce slag.

[1] LPG, Liquefied petroleum gas, In Swedish: Gasol

Direct Reduced Iron, DRI is produced from crushed or pelletised iron ore. If the ore is not pelletised, the reduced product is usually hot briquetted. This reduced product is called HBI, hot briquetted iron. Sponge iron is also used, as a complement to scrap as basic material in the process of making steel. Sponge iron powder is produced by reducing the oxygen in the iron ore at lower temperature with carbon monoxide and hydrogen. The world production is about 55 million tons (2004). Höganäs in Sweden produces sponge iron powder only for their use of iron powder [12-14].

2.2 Characteristic's of Steel

Steel is an iron alloy, with carbon as the primary alloying component. Carbon is used so regally that it does not count as a "real" alloy addition. To be able to form the steel, the alloy of carbon must not exceed 2 %. The amount of carbon has a fundamental significance on the quality of the steel. More carbon gives the steel better strength, while toughness and welding ability decreases. In the raw steel process components are added to achieve suitable quality of the steel, for example to decrease corrosion. Alloyed steel has fixed minimum levels for different alloy composition. Manganese, silicon, chrome and nickel are examples of alloy additions. For example a regular stainless steel so called 18/8 contains 18 % chrome and 8 % nickel. More than half of the Swedish steel production is alloyed steel, which is far more then in the rest of the world. Unalloyed steel has less content of alloy components than required for alloyed steel. Unalloyed steel is often merchandised as Handelsstål in Sweden [12].

Secondary steelmaking or ladle metallurgy describes the process that take place nearby the furnace where the liquid steel is refined. Desoxidation, possibility to adjust the alloys and control the casting temperature is done in the ladle. The liquid steel is often cast in a continuous casting machine. This is, however, not always suitable and in this case the older method, with a mould is used. The product is then called ingot. Cooling, heating and hardening can also change the quality of steel.

The largest amount of the steel works production is products that will be further worked and refined. The working of cast steel is performed to achieve the wanted form and quality. This is usually done by hot rolling and in some cases cold rolling or forging. The products can further be treated by heating, straightening, grinding and polishing. Large irregular details or very small details can be cast as finished details directly.

Rolling is the most widely used forming process in which the thickness of a material is reduced by passing it between two rolls, Figure 2. Hot-rolling is used to form larger amounts of deformation. Cold-rolling is used to optimise the mechanical properties and surface finish. Drawing is metal-forming operations where a piece of metal is pulled through a die in order to reduce the cross-section, see Figure 2. Rod, wire and tube are all produced by this process [12, 15].

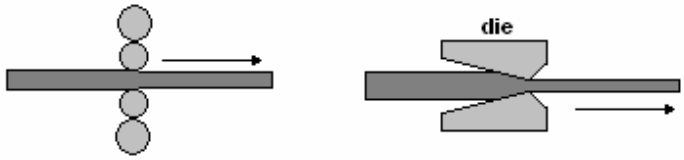

Figure 2. Rolling and drawing material are two ways to form the material.

Forging is a metal-forming operation where the workpiece is deformed between machine-driven hammers or hydraulic presses, see Figure 3. It is often used to form large details or details with irregular form. An example is the crankshaft on cars and ships. In closed die forging, smaller components are formed. The two halves of the die completely enclose the workpiece. In open die forging, the workpiece is free to elongate between the dies as the force is applied [12, 15].

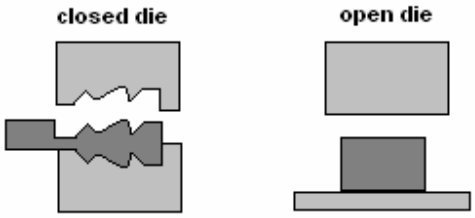

Figure 3. Forging can take place in either a closed or in an open die to form the metal.

3 Steel and the environment

Steel has been in an efficient cycle for a century. Raw material and energy are used in the steelmaking processes and results in products that people use in their daily lives. When the product has served out, it could be recycled and sold again as a new raw material, called scrap. There are also products that remain after the process is finished, which sometimes goes further to other cycles.

The Swedish steel industry is one of the leading in the world according to use of today's best process technology. New processes can give great improvement in process technology, raw material and energy use. Since the development of new processes demand great resources, Swedish steel industry depends on the developments in other countries. The new processes that are made on the experiment and demonstration state today are about a decade from being used in the industry. Most of the energy-saving efforts are done at the same time as a factory is doing new investments or larger rebuilding [12].

3.1 Energy and power

The word energy comes from Greek and means work. Energy is difficult to describe since it can't be seen or touched. Energy can be of different forms such as electric, heat, chemical, potential, mechanical or movement. Electric energy can be taken form the electric network. Chemical energy comes from oil, petrol, LPG etc. An example of mechanical energy is a rotating axle on an electric engine. The potential energy, happens when something is located higher up than the surroundings, for example the water in the pound above a hydroelectric power station. The binding energy of a particular electron is the energy, which would be required to remove it from the atom to an infinite distance. Kinetic energy or energy of movements is for example a moving car or a water stream [12, 26-27].

Some facts:

1. The energy can't be destroyed, only transformed.
2. All energy are sooner or later transformed into heat
3. Heat transports from higher to lower temperature, i.e. from warm to cold.

The power is said to be the energy per time unit. The power is measured in watt (W), and the energy in joule (J), where 1 J = 1 Ws (Watt-second)[2]. The energy is often measured in kilo-watt-hour (kWh). 1 Wh = 3600Ws. Some examples of how to estimate some energy contents, Table 1 [12]:

[2] Compare to electric conditions in chapter 4.3.

Table 1. Examples of energy contents in fuels.

1 kg oil	gives	about 41 MJ	or	11.4 kWh
1 kg LPG[3]	gives	about 46 MJ	or	12,8 kWh
1 kg coal	gives	about 7 MJ	or	7,6 kWh

Energy transformations:

Input energy = Output energy

Useful energy (%) + Energy losses (%) = 100 %
Efficiency h q (sometimes η) = Useful energy / applied energy.

There are losses in every energy transforms. Efficiency is used to examine how much of the applied energy that is transformed into useful energy. For example if half of the energy becomes useful the efficiency will be 50 %. When heating a metal in a furnace, the best would of course be if all the applied energy would be transformed into heat-energy in the metal, this is however impossible. Efficiency tells how much of the energy from the fuel that is transformed into heat in the material. An EAF plant usually has the thermal efficiency of about 60 %.

3.2 Energy consumption in the steel making process

Energy is and has always been and will probably even in the future be one of the most important production factors in the iron and steel industry. In the old days the iron works were placed by rivers, which gave waterpower and near woods that could provide charcoal. The majority of the steel works in Sweden is still in Bergslagen. The ore based (integrated) works dominate the energy consumption. This is because the coke for the reduction- and alloy components are also considered in the energy-balance. In a scrap-based work the electric energy is the most important, and since the steel scrap already is metal the reduction process can be excluded [12].

In the scrap steel making process the electric arc furnace, is the far biggest consumer of electricity. The electric arc furnace can have electric power of up to 80 000 kW. It takes 450-600 kWh electric energy to melt one ton of scrap. The voltage in the furnace is up to about 500 V, while the electric current is high; up to about 80 000 A and the frequency is 50 Hz. Fuel is mostly used in heating furnaces and boilers. Even in EAF fuel is used in oxy-fuel burners. In these, fuel is burnt with oxygen in special burners, in order to speed up the melting of the scrap. Even some amounts of carbon are inserted in the furnace to accomplish foaming slag, which lowers the electricity use in the furnace. All energy that has been provided has to leave the work in some way or another. Energy is transported away from the work in hot exhaust from furnaces and boilers, with cooling water, with

[3] Liquid petroleum gas, in Swedish; gasol.

the ventilation-air, through heat-losses in walls etc. Many steelworks sells the heat to communities nearby [12]. Figure 4 shows an overview of the flow of energy in the steel making process from scrap to finished products.

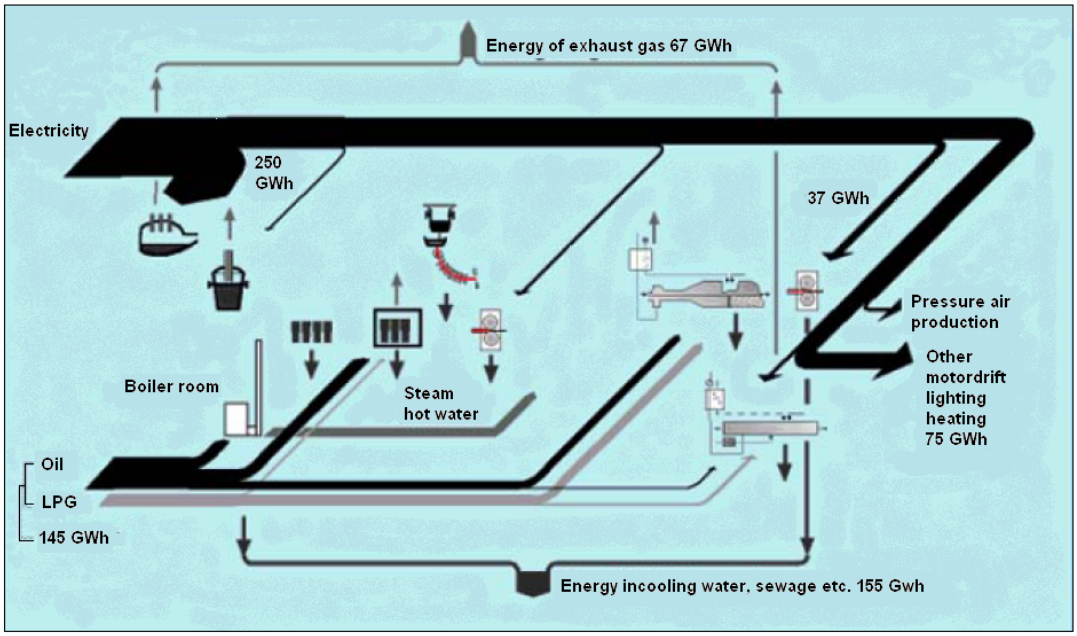

Figure 4. The energy flow in a scrap steelmaking process comes from various sources.

The majority of the energy-demanding processes in the steel industry take place at high temperatures. The energy is mainly used in processes with work-temperature over 1 000 ^{o}C. This relationship means that the steel work need high worthy energy carriers, like electricity, carbon- and oil products and gas (LPG or natural gas) to uphold the production. Today there is no possibility to use low-valued fuel, like bio-fuel, partly because the burning of oil and gas is in the same "room" as the material to heat. This means that there are big demands on atmosphere and the fuels ashes so that the quality of the steel isn't going to change. The coal can today not be replaces by any other energy-carrier, but there is technique to replace oil and gas by electricity [12].

Coke is mainly used in the reduction-processes, *i.e.*, in blast furnaces and sponge iron furnaces. Some of the coke can be replaced by charcoal powder, oil, tar, etc. The gas from the production of coke can be used in the rolling mills heat- and heat treatment furnaces and in boilers. The gas from the blast furnace is used to preheat the air in the blast furnace. Electricity is used for engines, scrap melting in electric arc furnaces and heating- and heat treatment in rolling mills. Some work has electric boilers. Although more electricity is used for automation and environment-investment has the specific electricity use per ton steel not become any higher. Oil is used in the rolling mills heating- and heat treatment furnaces and for local heating. The use of oil has decreased drastically since 1970, by numerous reasons; carbon-injection, instead of oil in the blast

furnace, a new casting technique that gives less heating in the rolling mills, closure of all martin-furnaces, LPG and more efficient use of energy. LPG (liquefied petroleum gas) is used in heating- and heating-treatment furnaces. In Sweden natural gas is used at a couple of constructions in Skåne and Halland, there it replaces oil. The use of rest-energies grows both inside the steel works and externally. It is in the first place the ore-based works that generate large amounts of rest-energies [12].

3.3 Rest-products

While producing steel various types of rest-products are also produced, for example slag and dust. Slag is a by-product formed in melting, welding, and other metallurgical and combustion processes and is formed by impurities in the metals or ore being treated. Slag consists mostly of salts formed by combination of basic oxides like calcium oxide (e.g. lime from limestone, ash, aluminum oxide) and acidic oxides of elements such as silicon, sulphur and phosphorus. Slag is less dense than metals so it floats on the surface of the molten metal, protecting it from oxidation by the atmosphere and keeping it clean. Slag can be used to produce a special type of concrete: It is used as a road material and ballast and as a source for available phosphate fertilizer [12, 15].

In a flue gas facility dust is separated as a rest product in either dry or wet condition. Usually dry methods are used, but sometimes the only alternative is a wet method, because the risk of explosion.

Emulsions, are used as lubrications and cooling matter in cold-rolling. In treat with acids iron oxide, iron sulphur or metal-hydroxide slams gets as rest products, depending on acid. When polishing to remove unevenness steel dust gets as rest product. The furnaces are lined with bricks, which has to be changed sometimes. Raw materials, which is to fine grained for original use is also a rest product. 60-70 % of the rest products are reused internally or externally. A certain amount is stored to later reuse or sale and the rest, about 30 % is deposited [12].

In the iron ore based works a large amount of the rest products are returned to the process. In works with sintering facilities the main part returns to them. SSAB in Sweden has not had a sinter work since 1995, and has therefore developed a technique where the rest products are reused in form of cement bounded briquettes to the blast furnaces [12].

4 Scrap

Recycling is no news for the steel industry. Since the 1900-century there has been methods to melt scrap and produce new steel products. Scrap is a natural and important raw material in modern steel manufacturing. Therefore there is a well known market, where scrap can be sold and bought according to agreed quality rules. Iron scrap is non-usable products, like scrap (and fragmented) cars, old machine-parts, which contains iron. In steel manufacturing, scrap comes from for example; plate-clip or metal chopped from the ends of ingots, see Figure 5. Even households leave cans and other metal to recycling. The cans are first heated to burn off etiquettes, color, plastic- and food rests. After that the metal is sorted, with magnetism for steel and vortex for aluminum. After sorting out the steel, it is transported to a steel work where it is melted down to new steel. Scrap is classified by chemical content and form [12, 16-18].

Figure 5. Examples of steel scrap.

The scrap comes from different sources and has a great variation both in physical an in chemical quality. The scrap can be one day old or 100 years old. The quality depends on where the scrap is coming from and when it was manufactured. Thousands of different kinds of steel to hundred thousands applications means that one piece of scarp very seldom looks like the other. This is why it is important to sort out the scrap in different groups, scrap-classes, so that the recycling gets as efficient as possible. A lot of research is going on both in the steel industry and the scrap industry to better sort the scrap quality and using the scrap more effective. Steel scrap is divided by quality in a large number of classes depending on origin, dimension and analysis.
The classes of scrap, together with rules for delivery, are described in a book (In Sweden Skrotbok [19]) for unalloyed scrap and for stainless steel. This is the result of voluntary agreement between scrap marketers and steel works. The classes are similar in different countries and works as a foundation for the common quality development between the scrap industry and the steel industry. Some examples of Swedish classification of steel scrap are shown in Appendix 1.

This is how a load of scrap is classified [16]: When the scrap comes to the recycling facility it is weighted and controlled and the sorting begins. The sorted scrap is then sent to melting, casting or iron works. But often the scrap has to be prepared. Complex, cable- and electricity scrap has to be sanitised from pollutant contents before recycling.

Complexed scrap, like cars, refrigerators and machines consists of various metals and other materials. Therefore it must be fragmentised before it can be sorted. In a powerful hammer mill the material is grinded into fist sizes. Magnets, air streams, water bathe and manual sorting separates the different materials. Paint and enamel on the metals are carved of almost completely during fragmentising. Paint that remains is burned away during melting in the furnace. The less paint left in the material, the less discharge from the furnaces. If the scrap is large and shapeless, so that it does not fit into the scissors it must be manually cut. Cutting is otherwise one way to work up the scrap to suitable size. In Gothenburg and Eskilstuna Sweden's larges scissors for cutting scrap are located their cutting-power are 1.000 tons [16]. Thin material can be pressed to compact packages (bales) to use in furnaces at steel works, foundry and melting works. From an economical and environmental view it is better to transport pressed material. Another way is to press metal chips into briquettes. The benefits with briquettes are that they are drier than loose chips and consist of less oils and emulsions, and they don't spatter in the furnaces [12, 16-17].

Cable often contains valuable metals like copper, aluminum and lead. To extract the metal the cable is treated in an advanced system. After sorting the cable is cut into decimeter long pieces to afterward be granulated. This means that it is grinded in several steps until it is so fine-grained that plastic and metal are separated. The granulate are then put on a vibrating separation table where the materials specific weigh decides when they fall of the table. Plastic falls of first, then alumina and at the end copper. After the scarp is sorted it is going back into the metal melting process [16].

5 Electric arc furnaces (EAF)

There are several processes for melting steel scrap. Today, the melting usually takes place in electrical furnaces, where the electric arc furnace is the most used. Electric current can be used for heating steel in three ways [20]:

1. By passing electric current through an ionised gaseous medium and using the heat radiated by the generated arc
2. By passing current through solid conductors and using the heat generated as a result of the conductors' inherent resistance to the flow of current.
3. By bombarding the steel surface with a high intensity electron beam and using the heat generated by the conversion of energy at the relatively small area of electron impingement.

The first practice, arc heating, can be applied through two methods;

- In **indirect-arc heating** arcs pass between electrodes supported in the furnace above the metal. In this method, the metal is heated solely by radiation from the arcs.
- In **direct-arc heating** arcs pass from the electrodes to the metal. In this method, the current flows through the metal charge so that the heat developed by the electrical resistance of the metal, though relatively small in amount, is added to that radiated from the arcs.

In direct-arc heating method, two types of furnaces are used: furnaces with **non conducting** bottoms, and furnaces with **conducting bottoms**. In a direct-arc furnace with a non-conducting bottom, the current (AC - alternating current) passes from one electrode down through an arc to the metal charge, through the metal charge and up through an arc to an adjacent electrode. In a furnace with a conducting bottom, the current (DC - Direct current) passes from an electrode down through an arc into the metal charge and then out of the furnace through an electrode forming part of the bottom in contact with the bath.

The second practice, resistance heating, can be applied through three methods;

- The Indirect method in which the steel is heated by radiation and convection from resistors through which the current is passed.
- The direct method in which current is passed directly from a power source through the metal.
- The induction method in which current is induced in the steel by an induction coil connected to a power supply.

Neither the indirect nor the direct method of resistance heating is practical for steel-melting operations. However, the induction method is employed successfully in special steel-melting applications. The steel charge in the induction method acts as the secondary circuit for current which is generated from a primary induction coil. The third practice has not been developed sufficiently for high tonnage capacities.

Numerous types of furnaces using electric current as the source of heat have been developed, but relatively few have survived as practical steelmaking tools. Among the types of electric furnaces, only three types has so far been proved to be practical in the industry for melting steel; the three-phase AC direct-arc, the DC direct-arc electric furnace and the induction furnace.

5.1 Direct-arc electric-furnaces

First some history of the direct-arc electric-furnace; Dr. Paul Heroult developed and patented the first AC direct-arc electric-furnace in the late 1800's. Aside from various innovations, developments and refinements in the design of the furnace components, the basic design principle remains the same as it was originally developed and patented. The primary concept for the furnace developed by Dr. Heroult involved the use of two or more electrodes, with the electric current passing from one electrode through an arc to the charge, then flowing through the charge and passing through an arc to the other electrode or electrodes. Accordingly, this type of furnace is often referred to as the "Heroult" type [13, 20].

The steel manufacturing in electric arc furnaces accelerated during the 1930 and 1999 were 33 % of the world production of raw steel produced in EAF. Depending on access to raw material, energy and technical development the scrap based metallurgy vary between different parts of the world. The amount of raw steel produced in EAF increases yearly by 4-5 % and is believed to be about 400 million ton 2005 and answer for more than 50 % of raw steel production 2010 [12]. The increase of minimills both in developing countries and the industrialised world contribute to the substantial increase together with investments in the existing steel industry. The cost of investment in electric arc furnaces technique is considerable smaller than for ore-based steel manufacturing. The ordinary electric arc furnace, Figure 6, consists of a cylindrical furnace room with basic lining [12, 20].

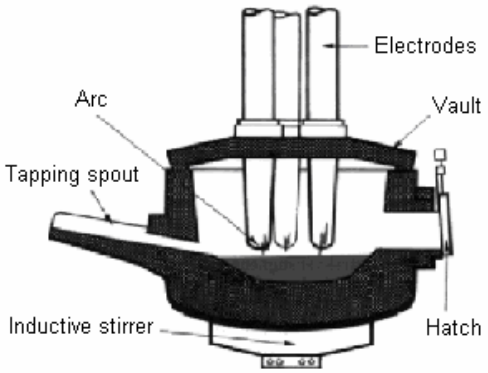

Figure 6. An AC electric arc furnace with 3 electrodes.

Figure 7 and Figure 8 presents the single electrode DC furnace at Mefos - Metallurgical Research Institute AB that is especially suitable for treatment of fine-grained material by charging through the hollow graphite electrode. The furnace is supplied with a 5 MVA transformer and an AC-DC thyristor-controlled rectifier. The furnace shell is water-cooled as are the roof, the gas outlet and the tap-hole area. The furnace is supplied by a transformer serving both the AC and the DC furnace. The 12 ton AC-furnace at Mefos (see Figure 10) is suitable for conventional scrap melting [21].

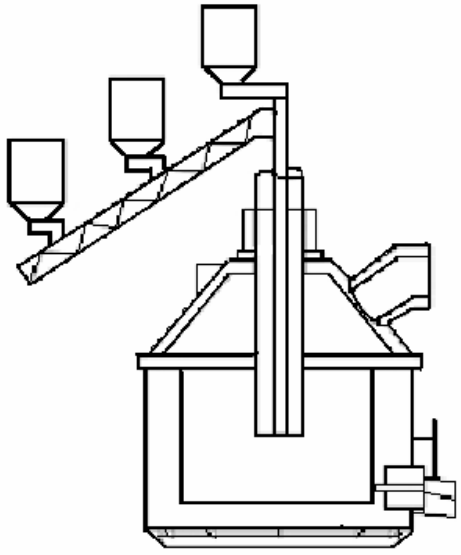

Figure 7. A principle sketch of the DC electric arc furnace.

It was believed that it would be better from an economical point of view with a DC furnace. A comparison of electrode use between AC and DC furnaces shows that the DC furnace uses 1-1.5 kg/ton steel and the AC furnace 2-3 kg/ton steel (even in some cases lower than 2 kg/ton steel). The difference in the cost of electrodes decreases because AC furnaces use electrodes 600 mm in diameter while DC furnaces use electrodes with 700-750 mm in diameter, which is about 20 % more expensive. The DC furnaces have higher costs for construction and maintenance work since it uses a bottom electrode, this is however in some way compensated by lower cost of electrode material. Both the inner and outer environment is affected by the sound level, when charging and when the power is on the furnace. A DC furnace gives 50-60 % less noise than an AC furnace, but different construction can decrease the difference [12, 22].

Figure 8. The five ton DC- electric arc furnace at Mefos- Metallurgical Research Institute AB.

The arc in an electric arc furnace is created in similar way as in arc-welding with one electrode. In arc-welding an electric current is passed through an electrode, which is brought close to the metal surface. When they get contact they melt together and when the electrode slowly removes from the metal an arc occurs. The heat from the arc melts the electrode onto the surface of the metal being welded [15]. When an electrode in an electric arc furnace gets in contact with the electric leading metal scrap, there will be a current in the circuit and when the electrode rises an arc occurs between the graphite electrode and the scrap. When the electrode has contact with the scrap the contact surface is heated. At high temperatures material is leaving the electrode in the form of charged ions [12-13, 22].

The arc can be divided in three different parts [13];

- Cathode-area (negative charge), which is a spot on the cathode where the arc starts.
- Arc, which contains of a conducting plasma[4]
- Anode-area (positive charge), where the arc ends.

[4] The arc is able of conducting current because the gas is in a condition called plasma. The condition occurs when a material is heated to many thousands degrees. In plasma is a significant amount of the electrons free, like in a metal which made plasma an excellent conductor. Of all the materials in the world 99% is in the plasma state[22].

In alternating current EAF (AC) the electrode and the scrap changes of being anode and cathode. In a direct current EAF (DC-furnace) is always the electrode cathode and the bottom of the furnace is anode. In a DC-furnace the bottom has to be a conductor [12-13, 22].

The heat transfers are mainly radiation from the arc to the scrap. In some part heating radiation comes from the heated ends of the graphite electrodes to the scrap. A convective heat transfer comes also from the arc [23]. The temperature in the middle of the arc is about between 10,000 ^{o}C and 30,000 ^{o}C [13].

The melting in an EAF can be divided into 5 different events [13, 22].

1. At start the furnace is filled with scrap and the electrodes have to work in the upper part of the furnace. The arcs are lighted and it is important to stabilize these and lover the points of the electrodes into the scrap.
2. Relatively soon the electrodes are bored down in the scrap, until they are a bit from the bottom of the furnace. The furnace in now working at medium high effect.
3. As the electrodes come closer to the bottom of the furnace a melt begins to form.
4. During the main part of the melting the electrodes are working with the highest possible power. The sides of the furnace are protected by scrap and have water-cooled panels. If more than one scrap bucket is charged the first steps is repeated.
5. When the main part of the scrap is melted and the temperature shall rise the power has to be reduced and the arc shortened to protect the furnace. During this time foaming slag can be used, which protects the walls and therefore use longer arc.

Stirring is of importance to equalize the temperature in the bath, especially in the peripheral parts of the bath. When continuous charging is used it is important to avoid lumps of not yet molten material. A DC-furnace will be electromagnetically stirred when the current is passing the bath, however this is sometime not enough, and other stirring is also used. The stirring can take place through gas injection by nozzles in the bottom of the furnace. An effective stirring is created if coal powder, (or fossil fuels) and oxygen is injected under the surface of the steel bath [12, 24]. Some furnaces are equipped with an inductive stirrer in the bottom of the furnace to for example make it easier tip the slag.

The furnace can be tilted forwards and backwards to simplify the tapping of steel and slag, see Figure 9 and Figure 10.

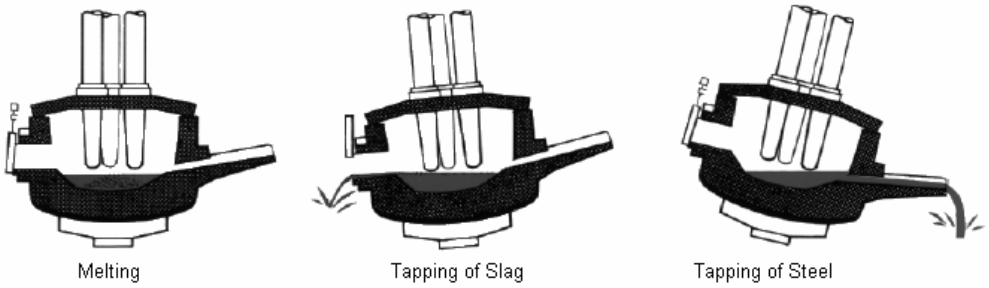

Figure 9. The furnace can be tilted to simplify tapping.

Figure 10. Tapping of the AC-furnace at Mefos – Metallurgical Research Institute AB.

5.2. Charging Scrap

The vault with the electrodes can be moved aside to enable charging, which often takes place in stages when a bucket of scrap is lowered into the furnace. The various types of scrap are placed in order to give an effective melting, see Figure 11. It is vital to have a cushion of light scrap at the bottom of each bucket. This acts as a cushion not only for the bottom of the bucket, but also for the bottom of the furnace to protect it from the damage, which can be caused from heavy lumps of scrap. This cushion can also act as a seal preventing very small pieces of scrap from being lost through the bucket bottom. Light scraps are also desirable at the very top of the bucket to facilitate leveling if the scrap is higher than the bezel ring on the furnace. This also allows the electrodes to quickly bore into the charge shielding refractory from arc damage and has a positive effect on the arc length, Figure 12. Heavy and large scrap must always go towards the bottom of the buckets for two reasons. First, if they are placed near the top of the bucket and fall

awkwardly during charging, they can stick up from the furnace causing excessive leveling delays. Secondly, heavy lumps which fall from high up in the furnace can easily cause electrode breakage simply from physical contact when they drop [22].

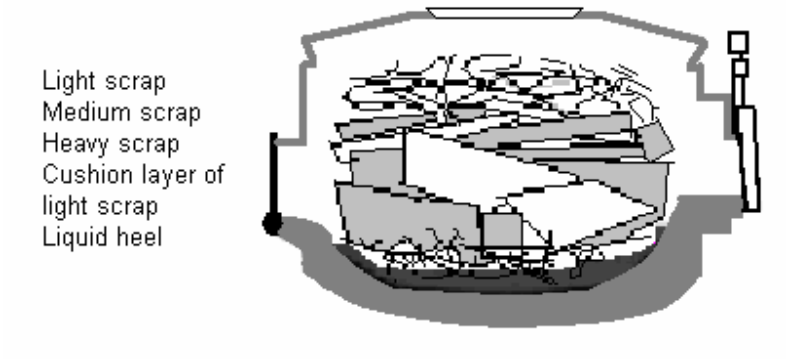

Figure 11. Correctly charged furnace.

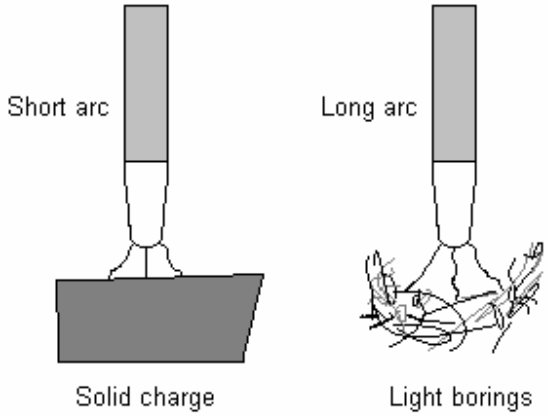

Figure 12. Effects of scrap type on arc length.

5.3. Voltage and Power

The plasma in the arc consists of gas molecules that has been ionised. Ionising happens when gas-molecules collide in very high speed, and electrons strikes loose from the atomic nucleus and positive gas molecules is formed. The electrons then accelerate towards the anode and the positive gas molecules towards the cathode. Since the electrons have easier to move they contribute most to the electric current. Nitrogen begins to ionise at temperatures over 4.000 ^{o}C. This relation is used in DC-furnaces, where the scrap is anode all the time. When the scrap is anode the temperature will come up to about 2.500 ^{o}C [13]. The drop of voltage over the arc can de divided in three areas, cathode, arc and anode. The drop of voltage over cathode- and anode-areas is

respectively in the size 25-30 V and 15-20 V and together about 50 V. The drop of voltage in the arc depends on arc-length and has been measured to 0.5-1.8 V/mm. In normal cases mean 1 V/mm is often used. This means that if voltage on 450 V is placed, it will be enough to an arc-length of about 400 mm (400 V for arc and 50 V for cathode and anode). With a longer arc between the electrode and the scrap the arc might drop off. Since most arc furnaces uses alternating current, this would mean that the arc would break when the voltage is zero, but because of natural inertia in the ion field there is no need for new contact between electrode and scrap. The voltage in the arc mainly depends of the length of the arc and degree of ionization. Scrap that falls to an electrode or a suddenly vaporizing of a metal therefore affects the voltage [13].

In a direct current circuit the power, P that develops over the resistance, R is given by [13, 25];

$$P = U \cdot I = R \cdot I^2. \quad (1)$$

The energy, E that emits over the time, t is

$$E = P \cdot t. \quad (2)$$

In transference of alternating current with high power over long distances the losses decreases through a large voltage and low currents. In difference to a direct current circuit the current and voltage are not constant, but vary normally after a sine shaped curve with frequency f, $f = 1/T$. Negative currents mean reverse direction. Through instantaneous reflections can alternating current be treated like direct current in the calculations, which means that in every point in time [13, 25];

$$p = u \cdot i. \quad (3)$$

When a current is changed in an AC-circuit, the circuit itself is trying to counteract that by producing a counter voltage, i.e. a reactance occurs. This can be explained by looking at a conductor, with current I. A magnetic field is formed around it. If the current is changed the magnetic field will also be changed, but the inertia of the magnetic field also gives an induced voltage in the conductor. This counter voltage will be proportional to time derivative of the current $\left(\frac{di(t)}{dt} \right)$ and the reactance X. The impedance represents the opposition, which the circuit exhibits to the flow of sinusoidal current. Although the impedance is the ratio of two phasors, it is not a phasor, because it does not correspond to a sinusoidal vary quantity.

The impedance as a complex quantity may be expressed in rectangular form as;

$$Z = R + Xj. \tag{4}$$

The reactance X is depending on the inductance and capacitance of the circuit. Because of the reactance the induced voltage is shifted 90^o towards the current in an AC furnace. This can be written as

$$i(t) = i_{\max} \cdot \sin(\omega t + \beta)\,. \tag{5}$$

The time derivative becomes

$$\frac{di(t)}{dt} = i_{\max} \cdot \omega \cdot \cos(\omega t + \beta) = i_{\max} \cdot \omega \cdot \sin(90^o + \omega t + \beta)\,. \tag{6}$$

The voltage over the resistance in the circuit $\left(u(t)_R = R \cdot i(t)\right)$ is in phase with the current. The total voltage becomes the sum of all these voltages and leads to a change in the phase between current and voltage. This means that the instantaneous power becomes negative in certain periods. When $p(t)$ is negative, power is absorbed by the source; that is, power is transferred from the circuit to the source. This is possible because of the storage elements in the circuit. When $p(t)$ is positive, power is absorbed by the circuit it is the active power that is used for the melting [13, 25].

The instantaneous power changes with time are difficult to measure. The average power is more convenient to measure. The average current *i(t)* and voltage *u(t)* for an AC-current is the value which in average gives the same power development over a (constant) resistance, like a corresponding DC-circuit, with current I and voltage U.
Effective value (Average value) [13];

$$I = \sqrt{\frac{1}{T}\int_0^T i(t)^2\,dt} \tag{7}$$

and

$$U = \sqrt{\frac{1}{T}\int_0^T u(t)^2\,dt}\,, \tag{8}$$

where T is the time of the period. For a sinusoid current respective voltage this gives $I = \frac{i_{\max}}{\sqrt{2}}$ and $U = \frac{u_{\max}}{\sqrt{2}}$, where i_{max} and u_{max} are the instantaneous extreme-values. This means that time-dependent functions for current and voltage can be written as

$$i(t) = i_{\max} \cdot \sin(\omega t + \beta) = I \cdot \sqrt{2} \cdot \sin(\omega t + \beta) \tag{9}$$

and

$$u(t) = u_{\max} \cdot \sin(\omega t + \alpha) = U \cdot \sqrt{2} \cdot \sin(\omega t + \alpha). \tag{10}$$

Where α and β is the voltage respectively the currents phasial angles and the angle in between is $\varphi = \alpha - \beta$. The power P can then be divided in the active power $P = U \cdot I\cos\varphi$ (W) and the reactive power $P = U \cdot I\sin\varphi$ (VA_r). $P = U \cdot I$ defines as the ostensible power (VA). The power factor $\cos\varphi$ tells how large amount of the voltage provide that sets over the resistance ($R + R_L$) and therefore creates active power. In an EAF three phase alternating current (individually shifted 120^o respectively 240^o) is normal and the average power of the furnace is: $P = 3UI\cos\varphi$. Normally only one phase is needed to look at [13, 22].

The impedance Z in an arc furnace can be divided in to: X, reactance in inductors and cables towards the arc, R, resistance in inductors, cables and electrode, R_L, resistance in the arc itself. R_L is directly dependent on length L. Even if reactance and resistance R are constant, R_L will vary since the arc moves back and forward over the scrap. This gives a variation of the impedance Z. If an electrode is dipped into the melt, R_L will be zero and the short cut impedance Z_k depends on resistance R and reactance X. If the length of the arc is increased until a break: $R_L \to \infty$ [13].

The AC furnaces use three phases, which is the usual current distribution. The reason for three electrodes with individual phase displacements between the electrodes on 1/3 period is that no reconnection needed. The current through one electrode is equivalent to the backwards current in the other two electrodes. This gives a balance in the system without reconnection, when the phases are united in a ground, for example the melting scrap in an EAF [22].Three electrodes and three phases give the power

$$P = 3 \cdot U \cdot I \cdot \cos\varphi. \tag{11}$$

6 Melting

Melting is a dissolution problem in which heat and mass transfer between liquid and solid phases take place. The melting rate can be controlled by heat transfer, mass transfer or coupled heat and mass transfer, depending on the chemical composition of the solid and liquid phases. Heat transfer (or heat) is thermal energy in transit due to a temperature difference. Whenever a temperature difference exists in a medium or between media, heat transfer must occur. This master thesis refers to three different types of heat transfer processes; conduction, convection and radiation [12, 26-27].

6.1 Conduction

In a solid, conduction comes mainly from two mechanisms, atomic and molecular activity, see Figure 13. In a molecule the atoms are vibrating because of the motion of heat around its state of equilibrium. Higher temperature is associated with higher molecular energies that mean more movement and when molecules collide, which they constantly do, the neighbour molecules are increasing their amplitudes, if they are moving with lower amplitude. The temperature rises and the heat is said to be lead from higher temperature to lower temperature. The calculation of the heat flux in a molecule is complicated, since the amplitudes are quantified [26-28]. In metal the conduction mainly take place with free electrons. The free electrons can easily move in the metal and interact with each other and the atoms of the metal lattice by collisions. When that happens the energy is equalized in the material. The leading abilities follow each other, since the ability to lead electricity is using the same mechanism as heat transfer. Both capacities is decreasing with high temperature, since the electrons ability to move is decreasing, when they are spread through the lattice of the atoms, which vibrations gets higher amplitude with higher temperature. Conduction with free electrons is 100 times more efficient then conduction with lattice swaying [26, 28].

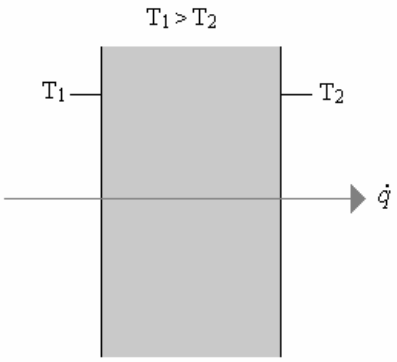

Figure 13. Conduction through a solid or a stationary fluid.

6.2 Convection

The convection heat transfer mode is comprised of two mechanisms. In addition to energy transfer due to random molecular motions (diffusion), energy is also transferred by the bulk, or macroscopic, motion of the fluid. This fluid motion is associated with the fact that, at any instant, large numbers of molecules are moving collectively or as aggregates. Convection heat transfer may be classified according to the nature of the flow. Forced convection occurs when the flow is caused by external means, such as by a fan, a pump or atmospheric winds, Figure 14. In contrast, for free (or natural) convection heat transfer the flow is induced by buoyancy forces, which arise from density differences caused by temperature variations in the fluid. Convection can be described as a heat transfer mode as energy transfer occurring within a fluid due to the combined effects of conduction and bulk fluid motion [26-27].

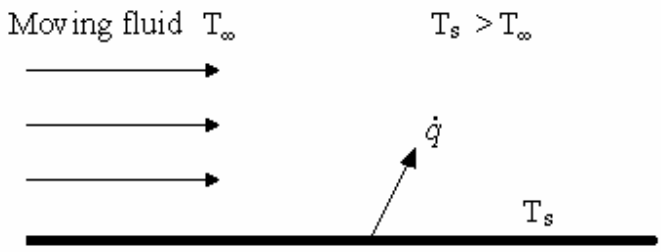

Figure 14. Convection from a surface to a moving fluid.

6.3 Radiation

Thermal radiation is energy emitted by matter that is at a finite temperature. Regardless of the form of the matter, the emission may be attributed to changes in the electron configuration of the constituent atoms or molecules. The energy of the radiation field is transported by electromagnetic waves (or alternatively, photons), see Figure 15. While the transfer of energy by conduction or convection requires the presence of a material medium, radiation does not. In fact, radiation transfer occurs most efficiently in vacuum [14].
Every electromagnetic wave can be characterized by wavelength λ and frequency *f*. In vacuum this gives [27]

$$\lambda f = c \ . \tag{12}$$

The thermal radiation is in $0.1 \le \lambda \le 1000\,\mu\text{m}$, and the visible part in 0.35-0.75 μm.

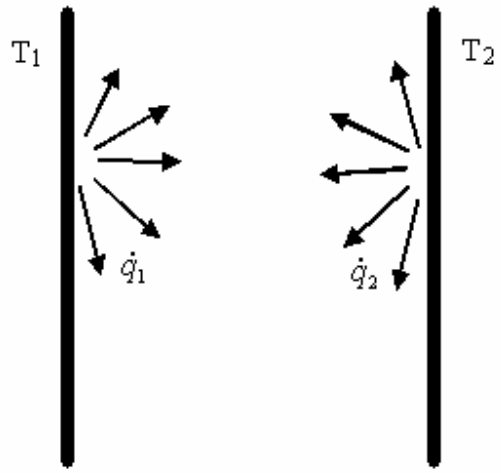

Figure 15. Net radiation heat exchange between two surfaces.

6.4 Melting in a melting furnace

The melting in an electric arc furnace can be divided in three stages, see Figure 16, [4-6];

1. Heating stage: The scrap is heated by the arc at the top of the furnace. The heating is carried out by both radiation and convection from the hot gases, which is going through the gaps between the scraps, and by conduction due to contacts among the scraps. The temperature of the scrap metal at the top increases until the melting temperature is reached. During this stage, only the gas-solid phase is to be considered.

2. Melting stage: As soon as melting begins, which happens first at the top, molten liquid drips down toward the bottom of the furnace. Thereafter the molten liquid level rises, while the height of the scrap metal decreases. The whole lump of scrap metal is heated by both the flame from the burners at the top and the molten liquid at the bottom. The liquid surface moves upwards as melting proceeds. The gas-solid and solid-liquid phases now exist simultaneously.

3. Finishing stage: Once the scrap metal is completely immersed into the molten liquid, only the solid-liquid phase is left. The domain to be considered becomes fixed. The molten liquid region broadens, while the solid-liquid region shrinks until the scrap is completely melted.

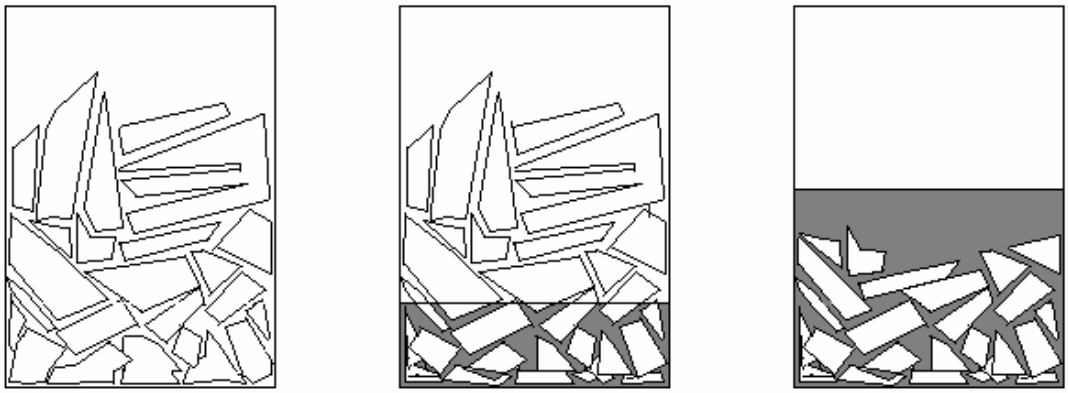

Figure 16. The three stages of melting.

7 Mathematical model of melting

In general, numerical simulations commonly used for phase change problems are classified into two different approaches: the fixed-grid and the transformed-grid methods. The fixed-grid method uses a single set of conservation equations and boundary conditions for the whole domain comprising the solid and liquid phases, while the transformed-grid method employs the governing equations based on the classical Stefan formulation. The interface conditions, therefore, are accounted for differently according to the method incorporated in solving the phase change problem. In the transformed-grid method, they are easily imposed because the interface is explicitly solved. However, in the fixed-grid method, the interface conditions are described as suitable source terms in the governing equations. A nodal latent heat value is assigned to each computational cell according to its temperature or enthalpy. Upon phase changing, the latent heat absorption, or evolution, is reflected as a source, or sink term in the energy equation.

When melting steel in a liquid steel bath, where the bath has a temperature of T_L, the initial temperature of the solid steel is uniform at T_0, and after immersion, the interface acquires the melting temperature of T_m. The traditionally used melting equations written in one dimension [3] are

$$h\left(T_L - T_m\right) = \rho L_f - k_s \frac{\partial T}{\partial x}\Big|_{\text{int}} \tag{13}$$

and

$$\frac{\partial}{\partial x}\left(k_s \frac{\partial\left(C_p T\right)}{\partial(t)}\right), \tag{14}$$

where k_s is the thermal conductivity, defined only in the solid steel, ρ is the mass density in the solid steel, C_p is the specific heat in the solid steel, h is the heat-transfer coefficient between the liquid and solid, L_f is latent heat of melting and v is the moving velocity of the interface (melting rate). Eq. (13) represents the heat balance at the interface, and Eq. (14) describes the heat conduction in the solid steel.

7.1 Enthalpy-porosity method

The fixed-grid method requires the velocity suppression because as a liquid region turns solid, the zero-velocity condition should be satisfied. The velocity suppression can be accomplished by a large value of viscosity for the solid phase or by a suitable source term in the momentum equation to model the two-phase domain as a porous medium. The fixed-grid method combined with the porous medium method is usually referred to as the

enthalpy-porosity method. The Enthalpy-porosity method example is taken from article [4-6].

7.1.1 Heating stage

To simulate the melting process in a circular scrap melter a simplified one-dimensional heat transfer model is built using enthalpy formulation and porosity to describe scrap geometry. Scrap metal is filled in a cylindrical furnace with height H and diameter D. The burner is located at the top of the furnace. The peripheral surface and the bottom are adiabatic [4].

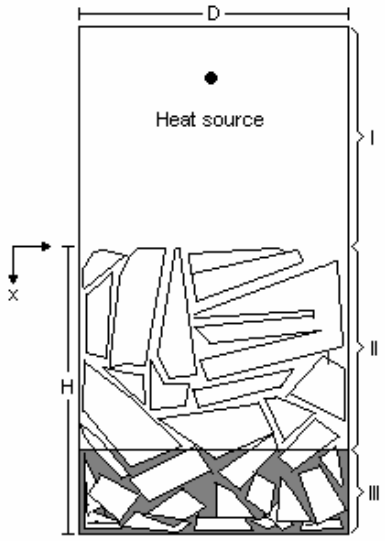

Figure 17. Schematic representation of the three regions of a melting furnace.

During the heating stage, described in 6.3 there is no liquid metal present in the furnace. The third region does not exist. Only the second region, the solid-gas phase, is to be considered. As it is impossible to solve the fluid flow and heat transfer within each individual gap between the scraps, the lump of scrap metal is treated as a pseudo-porous medium. As a result, the heat transfer mechanisms consist of heat conduction from contacts between the scraps is accounted for by invoking a porosity factor. Heat transfer by gas flow and radiation from the flame is included into a source term.

With the foregoing considerations, the governing equation for the melting of scrap metal may be stated as follows

$$\rho c_p \frac{\partial T}{\partial t} = \frac{\partial}{\partial x}\left(K \frac{\partial T}{\partial x} \right) + q \tag{15}$$

where, q is the heat source density and K is the bulk thermal conductivity. K is a function of the porosity;

$$K = k_s(1 - \delta_i) \tag{16}$$

where k_s is the conductivity of the solid and δ_i is the porosity, subscript i denotes gas or molten liquid by g or l, respectively. ρ and c_p are calculated in similar way as K. ρ is in reality ρ_{eff};

$$\rho_{eff} = \rho(1 - \delta_i). \tag{17}$$

$\delta_g = 1$, mean that the space in the porosity is filled with gas only, and $\delta_g = 0$ means that the space is filled with solid. The same is denoted in liquid, $\delta_g = 1$ space filled with liquid and $\delta_g = 0$ for a space filed with solid.

Region III (Figure 17) appears when the melting starts. The convective heat transfer from the molten liquid metal is taken into account by this new source term;

$$q_x h_l A_{eff}(T_b - T) \tag{18}$$

h_l is convective heat transfer coefficient of the liquid metal, A_{eff} is effective area and T_b is bulk temperature of the liquid metal.

When the whole scrap metal is immersed into the molten liquid (Figure 18), the second region disappears, and the last stage begins. The first region is the same as in the previous stage. The second region II' is a single phase (molten liquid), and the third region III' is the solid-liquid phase. In the liquid metal region the bulk thermal conductivity in Eq. (15) becomes the conductivity of the liquid metal, i.e., $K = k_l$. In the solid liquid region the governing equation remains unchanged, except for the bulk thermal conductivity, which becomes $K = k_l$. In the solid liquid region the governing equation remains unchanged, except for the bulk thermal conductivity, which becomes $K = k_s(1 - \delta_l)$.

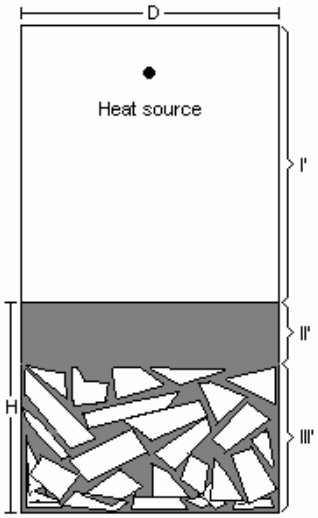

Figure 18. When the whole scrap metal is immerged into the molten liquid, three new regions of a melting furnace occur.

7.1.2 Enthalpy method

Taking advantage of the axisymmetric geometry of the furnace and heating from the top, the phase change problem may be formulated in terms of a one-dimensional time-dependent model. An enthalpy-based method is retained and leads to the following energy equation for the total enthalpy, H [4-6]

$$\frac{\partial H}{\partial t} = \nabla\left(K\nabla T\right) + q\,. \tag{19}$$

The total enthalpy is further split into sensible enthalpy and latent heat components, *i.e*.

$$H = h + \rho f_l L\,. \tag{20}$$

L is latent heat of fusion and h is sensible enthalpy, defined as

$$h(T) = \int_{T_m}^{T} \rho c_p dT\,, \tag{21}$$

where T_m is the melting temperature. The discrete form of the enthalpy-temperature

relationship is [4-6]

$$\begin{aligned} T &= T_m + \frac{H - \rho L}{\rho c_p} \quad H \geq \rho L \quad \text{(liquid phase)} \\ T &= T_m \qquad 0 \leq H \leq \rho L \quad \text{(mushy phase)} \\ T &= T_m + \frac{H}{\rho c_p} \qquad H \leq 0 \quad \text{(solid phase)} \end{aligned} \tag{22}$$

The local liquid fraction f_l I Eq. (20), is defined as

$$\begin{aligned} f_1 &= 1 \quad T > T_m \\ f_2 &= 0 \quad T < T_m \end{aligned} . \tag{23}$$

Substitution of Eqs. (20) and (21) into Eq. (19) yields

$$\rho c_p \frac{\partial T}{\partial t} = \frac{\partial}{\partial x}\left(K \frac{\partial T}{\partial x} \right) - \rho L \frac{\partial f_l}{\partial t} + q \,. \tag{24}$$

The potential advantage of this formulation is that the energy equation is cast into a standard form and the problems associated with the phase change are isolated in a source term (second term in Eq. (24)). q represents a heat source. The heat flux is normally known over the top of the charge. However, as the flame penetrates deeper inside the gaps, the heat source decreases along its axis exponentially. It is assumed that this damping effect of the heat source follows the relation [4-6];

$$q_x = q_0 e^{-\beta x} . \tag{25}$$

Here q_0 is the heat source value on top of the scraps, and β, the flame blocking factor, is a function of porosity,

$$\beta = \gamma \frac{2 - \delta_g}{\delta_g} , \tag{26}$$

where γ, the flame damping factor, describes the dynamics of the flame independently of the porosity of the scrap. The larger γ, the faster the flame vanishes along its length. The value of γ depends on the fuel's combustion rate as the fuel moves along the axis of the flame. Consider the following particular cases [4];

- If $\delta_g = 1$, which denotes a vacancy space, $\beta = \gamma$; then $q_x = q_0 e^{-\gamma x}$, which describes an unobstructed flame. This corresponds to the first and the second region (Fig.25).
- If $\delta_g = 0$, which means a completely solid region, $\beta \to \infty$; $q = 0$. The source term disappears. This corresponds to the pure conduction case.
- If $0 < \delta_g < 1$, $\beta = \gamma \dfrac{2 - \delta_g}{\delta_g}$. The source term decreases exponentially as the gas flows down into the gaps. This corresponds to the pseudo-porous media in region II of Figure 17.

7.1.3 Numerical Schemes

The discretised equations are obtained by integrating the governing equation, Eq. (24), over the control volumes. The resulting finite difference equation has the general form [4-6];

$$a_W T_W + a_P T_P + a_E T_E = Q. \tag{27}$$

Eq. (27) can be solved using a tridiagonal matrix algorithm (TDMA) method (Appendix 4). The simulation begin with initial temperature T_0 prevailing throughout the scrap metal. During the heating stage, there is no liquid metal in the furnace so the liquid fraction f_l is set to zero. Once the melting starts, the liquid fraction needs to be evaluated. In the computation, the discretised equations have the form

$$a_P T_P = -a_E T_E - a_W T_W + \frac{\left(f_P^0 - f_P^k\right)L}{c_p} + T_P^0 + \frac{\Delta t}{\rho c_p} q_0 e^{-\beta x}. \tag{28}$$

If phase change occurs at point P, I.e. $0 < f_l < 1$, the liquid fraction needs to be updated such that iteration $(k + 1)$ will become

$$a_P T_m = -a_E T_E - a_W T_W + \frac{\left(f_P^0 - f_P^{k+1}\right)L}{c_p} + T_P^0 + \frac{\Delta t}{\rho c_p} q_0 e^{-\beta x}. \tag{29}$$

Subtracting Eq. (28) from Eq. (29) results in the following liquid fraction update formulation:

$$f_l^{k+1} = f_l^k + \frac{a_P\left(T_P - T_m\right)}{L / c_p}. \tag{30}$$

Since melting starts from the top of the scraps and the height of the scraps decreases as melting proceeds, the origin of the x axis moves with the scrap height so as to maintain the control volumes in the same coordinates. Once a control volume is melted, the liquid metal is assumed to drip down to the bottom of the furnace. Indeed, observations made in a full-scale industrial melter have revealed that almost all of the molten materials from the top of the charge falls directly to the bottom to the furnace, since the spaces between the scraps are much larger than the molten film thickness. As a result, the third region appears. The incremental depth of the molten liquid is evaluated by [4-6];

$$\Delta l = \frac{1-\delta_g}{\delta_l}\Delta x, \tag{31}$$

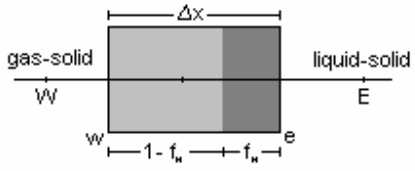

Figure 19. Control volume at the interface.

where Δx is the height of the control volume at the previous time step.

While the molten metal level increases, the height of the scraps decreases.
A control volume is completely immerged by the molten liquid, when

$$\begin{aligned} K &= (1-\delta_l)k_s \\ f_P &= 1 \\ q_x &= h_l A_{eff}(T_b - T) \end{aligned} \quad . \tag{32}$$

If a control volume is partially immerged by the molten liquid, as shown in Figure 19, then the source term may be expressed by

$$q_x = (1-f_H)q_0 e^{-\beta x} + f_H h_l A_{eff}(T_b - T). \tag{33}$$

As soon as the scrap metal is immerged completely into the molten liquid, the computational domain becomes fixed. The simulation becomes that of melting of a porous medium. In the second region shown in Figure 18, heat conduction prevails in the liquid metal. Therefore, $K = k_l$, $f_P = 1$, and the internal source term disappears. The

interface between the solid scrap and molten liquid will move downward according to the total enthalpy of control volumes until the solid scrap metal is completely melted into the liquid [4-6]. Density is assumed the same for liquid and solid. [4-6] used pure aluminum but mean that it would work for different alloys.

7.2 The CE/SE method

The method of space-time conservation element and solution element (CE/SE) was developed by Chang and To (1991) and Chang, Wang and Chow (1998) at the NASA Glenn Research Center in order to solve the conservation laws. Since its inception 15 years ago, the method has been found capable of accurately resolving shock waves and contact discontinuities without introducing numerical oscillations [7].

Apart form the established methods at the core of its development it has two basic beliefs [7];

- The first is that, in order to capture physics more efficiently and realistically, the modeling focus should be placed on the original integral form of the physical conservation laws, rather then the differential form. The latter form follows from the integral form under the additional assumption that the physical solution is smooth, an assumption that is difficult to realize numerically in a region of rapid change, such as a boundary layer or a shock.

- The second belief is that, with proper modeling of the integral and differential forms themselves, the resulting numerical solution should automatically be consistent with the properties derived from the integral and differential forms, e.g., the jump conditions across a shock and the properties of characteristics. Therefore a much simpler and more robust method can be developed by not using the above derived properties explicitly.

Currently, the field of computational fluid dynamics (CFD) represents a diverse collection of numerical methods, with each of them having its own limitations. Generally speaking, these methods were originally introduced to solve special classes of flow problems. Development of the CE/SE method is motivated by a desire to build a brand new, more general and coherent numerical framework that avoids the limitations of the traditional methods [7].

The problem formulation uses the enthalpy method and then the CE/SE method is described for numerical simulation of axisymmetric phase change problems using unstructured meshing, which is selected because of its flexibility for handling complex geometries. Effects of convection in melt are ignored in this formulation. The example of space-time conservation element and solution element method is taken from [8-10].

7.2.1 Governing equation, enthalpy method

The enthalpy method is used for modeling heat conduction with phase change phenomenon. This method gives the solid-liquid interface as a part of the solution without explicit tracking. The governing equation, i.e., the conservation of energy, with the assumption of constant thermophysical properties within each phase is the Fourier-Biot equation (Appendix 4) that, in axisymmetric form is written as, [9];

$$\rho c \frac{\partial T}{\partial t} = k\left(\frac{\partial^2 T}{\partial r^2} + \frac{1}{r}\frac{\partial T}{\partial r} + \frac{\partial^2 T}{\partial z^2} \right) + \dot{q}, \tag{34}$$

where r, z represents the radial and axial coordinates. In two-dimensional Cartesian coordinates [8];

$$\rho c \frac{\partial T}{\partial t} = \frac{\partial}{\partial x}\left(k\frac{\partial T}{\partial x} \right) + \frac{\partial}{\partial y}\left(k\frac{\partial T}{\partial y} \right) + \dot{q}, \tag{35}$$

where c, k, and ρ are specific heat, thermal conductivity and density of the material, respectively, and $\dot{q}$ refers to a distributed heat source that may be present in the domain, e.g., an electrical heating element. The left hand side of Eq. (34) and Eq. (35) is related to the change of enthalpy. The enthalpy may be defined as

$$\bar{h} = \int_0^T c dT + \phi L_f, \tag{36}$$

where L_f is the latent heat of fusion and ϕ equals 1 for liquids and 0 for solids. See also chapter 7.1. Using the above definition, Eq. (34) and Eq. (35) can be written as

$$\frac{\partial H}{\partial t} = k\left(\frac{\partial^2 T}{\partial r^2} + \frac{1}{r}\frac{\partial T}{\partial r} + \frac{\partial^2 T}{\partial z^2} \right) + \dot{q}, \tag{37}$$

and

$$\frac{\partial H}{\partial t} = \frac{\partial}{\partial x}\left(k\frac{\partial T}{\partial x} \right) + \frac{\partial}{\partial y}\left(k\frac{\partial T}{\partial y} \right) + \dot{q} \tag{38}$$

respectively, where $H = \rho\bar{h}$ is the enthalpy per unit volume. To use the above equation when both solid and liquid phases are involved, procedures are needed for both choosing the thermal conductivity and calculating the temperature field from the enthalpy field. Since *c* is assumed to be constant within each phase, the enthalpy of the liquid and solid, for a material that changes phase at a single temperature T_f, can be calculated from Eq. (36) as

$$\begin{aligned} H_s &= \rho_s\left(\int_0^T c_s dT\right) = \rho_s c_s T \\ H_l &= \rho_l\left(\int_0^{T_f} c_s dT + \int_{T_f}^{T} c_l dT + L_f\right) = \rho_l\left(c_s T_f + c_l\left(T - T_f\right) + L_f\right) \end{aligned}, \tag{39}$$

where subscripts *l* and *s* refer to liquid and solid phases, respectively. Therefore, the temperature field can be calculated using Eq. (39) as follows

$$T = \begin{cases} \dfrac{H}{\rho_s c_s} & H \le H_{sf} \\ T_f & H_{sf} \le H \le H_{lf} \\ \dfrac{\left(H - H_l f\right)}{\rho_l c_l} + T_f & H \ge H_{lf} \end{cases}, \tag{40}$$

where

$$\begin{aligned} H_{lf} &= \rho_l\left(c_s T_f + L_f\right) \\ H_{sf} &= \rho_s c_s T_f \end{aligned} \tag{41}$$

are enthalpies of the fusion liquid and fusion solid, respectively. These values can also be used in the numerical approach for determining whether each grid element is solid, liquid or undergoing melting/freezing. Corresponding thermal conductivities are then chosen for that grid element. For elements that are undergoing fusion, an average thermal conductivity is used. This average can be either the arithmetic average of solid and liquid values or a linear interpolation between them based on the value of *H*, both resulting in good simulations [9-11].

7.2.2 Numerical method: CE/SE

Consider the following partial differential equation, which can represent a variety of conservation laws depending upon the definition of *H* and the flux functions *F* and *G*

$$\frac{\partial H}{\partial t}+\frac{\partial F}{\partial x_1}+\frac{\partial G}{\partial x_2}=0\,, \tag{42}$$

where x_1 and x_2 are coordinates of a two-dimensional Euclidean system.
The axisymmetric governing equation, Eq. (37) can also be written in the form of Eq. (42). An alternative approach is used since the direct approach does not lead to a stable numerical method. The term $\frac{1}{r}\frac{\partial T}{\partial r}$ in Eq. (37) is treated as a source term and $x_1 \equiv r$ and $x_2 \equiv z$

$$\frac{\partial H}{\partial t}+\frac{\partial}{\partial r}\left(-k\frac{\partial T}{\partial r}\right)+\frac{\partial}{\partial z}\left(-k\frac{\partial T}{\partial z}\right)=\frac{k}{r}\frac{\partial T}{\partial r}\,. \tag{43}$$

Or, in general form similar to Eq. (42)

$$\frac{\partial H}{\partial t}+\frac{\partial F}{\partial r}+\frac{\partial G}{\partial z}=\widetilde{S}\,, \tag{44}$$

where $\widetilde{S}=\frac{k}{r}\frac{\partial T}{\partial r}$ represents the source term, and the flux functions *F* and *G* are defined as $F=-k\frac{\partial T}{\partial r}$ and $G=-k\frac{\partial T}{\partial z}$.

Considering (*r*, *z*, *t*) as coordinates of a three-dimensional Euclidean space-time, Eq. (44) can be written as [10];

$$\vec{\nabla}\cdot\vec{U}=\widetilde{S}\,,\ \vec{U}=\left(F,G,H\right). \tag{45}$$

Consider the two-dimensional Cartesian version, Eq.(38) in the *xy*-plane, with no generation. The governing equation for this case can be written in the above form defining for example [9];

$$F = -k\frac{\partial T}{\partial x},\ G = -k\frac{\partial T}{\partial y}. \tag{46}$$

When considering (x, y, t) as coordinates of a three-dimensional Euclidean space-time, Eq. (42) can be written as

$$\vec{\nabla}\cdot\vec{U} = 0,\ \vec{U} = \left(F, G, H\right). \tag{47}$$

A two-dimensional, unstructured, space-time mesh is used here which consists of Delaunay triangulation (Appendix 4) on the xy-plane that, considering the time axis as the third dimension, makes prisms perpendicular to the xy-plane, see Figure 20. C is the geometric centre of the hexagon $C_1C_2C_3V_1V_2V_3$ and the triangle $V_1V_2V_3$ [7, 9].

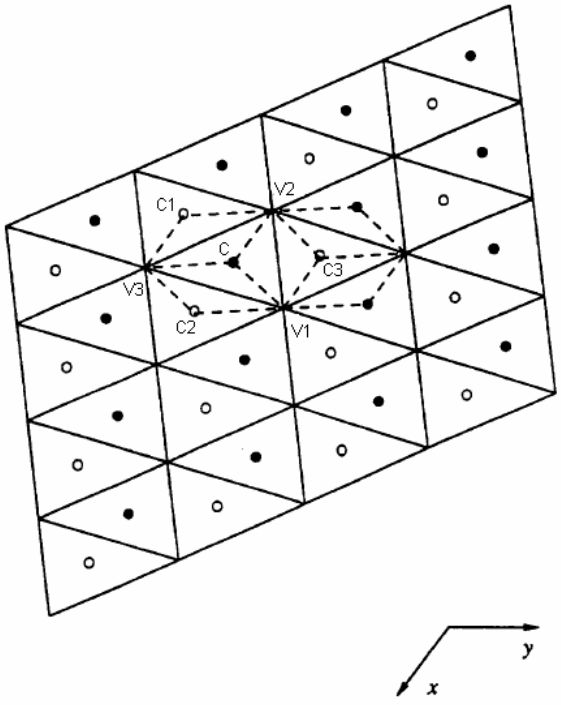

Figure 20. A spatial domain formed from congruent triangles, showing the spatial projections of the mesh points [7].

The computational molecule of this grid is shown in Figure 21 in the xy-plane, where nodes V_1, V_2 and V_3 determine vertices of a triangular cell j at time level n-½. Points C_1, C_2 and C_3 denote the centroids of three neighboring cells j_1, j_2 and j_3, respectively. Primed

points represent the same spatial nodes after half time-step. For each cell, the integral form of the governing equation, Eq. (47) may be applied to the octahedral element that is the union of three tetragonal prisms $CV_2C_1V_3V_3'C'V_2'C_1'$, $CV_3C_2V_1V_1'C'V_3'C_2'$ and $CV_1C_3V_2V_2'C'V_1'C_3'$. The octahedron will be called the conservation element (CE) of cell j [7, 9].

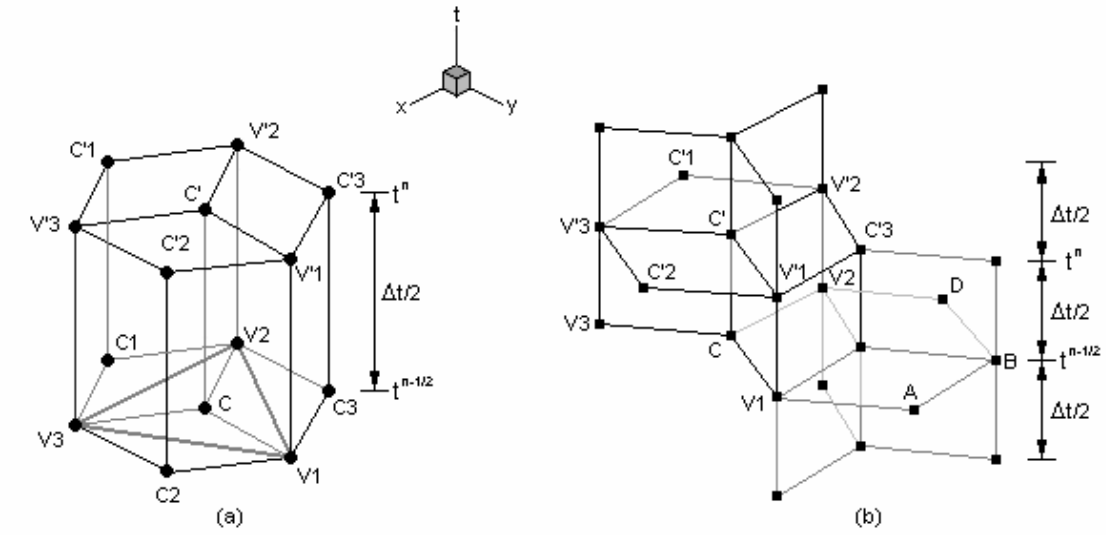

Figure 21. A computational molecule of CE/SE method, (a) CE's and (b) SE's.

The integral conservation law will then be

$$\int_{V(CE)} \vec{\nabla} \cdot \vec{U}\, dV = 0, \tag{48}$$

where $V(CE)$ denotes the volume of the conservation element. Divergence theorem (Appendix 4) on Eq. (48) gives;

$$\int_{S(CE)} \vec{U} \cdot \hat{n} ds = 0, \tag{49}$$

where S(CE) denotes the surface of the conservation element and $\tilde{n} = (n_x, n_y, n_t)$ in a and is the unit outward normal to it. To perform the integration of Eq. (49) $\vec{U}$ would be replaced by a first order Taylor series approximation (Appendix 4) about a suitably chosen node, the solution point, where the discretised values of $\vec{U}$ and its derivatives are

saved. In this method both $\vec{U}$ and its first-order derivatives are considered as the independent variables, which must be determined. By "suitably chosen" it is intended that, solution points may be selected such that the method is explicit, this will be shown later. [22] Let (x_j', y_j') represent the spatial coordinates of the solution point related to cell j.

Therefore, components of $\vec{U}$ may be approximated as

$$H(x,y,t;j,n) = H_j^n + (H_x)_j^n(x - x_j') + (H_y)_j^n(y - y_j') + (H_t)_j^n(t - t^n). \tag{50}$$

$H(x,y,t;j,n)$ is the value of H at the point (x,y,t) using entity (j,n). The same approach may be used for *F* and *G*. Further, the derivatives of *F* and *G* can be found from Eq. (46), *i.e.*

$$\begin{aligned} F_x &= -kT_{xx}, \quad F_y = -kT_{xy}, \quad F_t = -kT_{xt}, \\ G_x &= -kT_{yx}, \quad G_y = -kT_{yy}, \quad G_t = -kT_{yt}, \end{aligned} \tag{51}$$

where T_{xx}, T_{xy}, T_{xt}, T_{yx}, T_{yy}, and T_{yt} are second-order derivatives of temperature and their mesh values will be calculated later in the section of second-order derivatives.

Each node on any of the surfaces indicated in Figure 21a may be evaluated using different discrete values, e.g. the value of $\vec{U}$ at a point on the $CV_1V_1'C'$ plane may be found using the expansion point of cell j at time level n as well as time level n –½. Also the value of $\vec{U}$ at a point on the $CV_2C_1V_3$ plane may be found using the expansion point of cell j at time level n – ½ as well as that of the neighboring cell, j_1. To assign a unique value to each node while integrating, each surface needs to be related to one and only one (j, n) entity, which is called a solution element. Consequently, these entities must be defined as a combination of non-overlapping surfaces that decompose the entire domain. Figure 21b shows two of four solution elements related to the cell j, i.e. SE(j, n), which consists of the hexagon $C_1'V_3'C_2'V_1'C_3'V_2'$ combined with three vertical rectangular planes cutting through it, SE (j_3, n – ½) that consists of the hexagon CV_1ABDV_2 combined with three vertical rectangular planes cutting through it, where A, B, and D are related to the neighbour j_3 of cell j (not shown), and two other SE's (j_1, n – ½) and (j_2, n – ½) that are built the same way.

Consider the SE(j_1, n – ½). The area of two lateral faces related to this SE, i.e. $C_1V_2V_2'C_1'$ and $C_1V_3V_3'C_1'$ (Se Figure 21a) will be referred to as $S^{(1,1)}$, and $S^{(2,1)}$, respectively, while $\hat{n}^{(1,1)}$, and $\hat{n}^{(2,1)}$ represent the unit normals of the above lateral faces, outward with respect to the octahedron. Furthermore, spatial coordinates of the centroid of each of these faces will be referred to as $(x_c^{(1,1)}, y_c^{(1,1)})$, and $(x_c^{(2,1)}, y_c^{(2,1)})$, respectively.

Also the area of $C_1V_3CV_2$, that is the horizontal plane related to this SE, will be called $S^{(1)}$ while (0, 0, -1) represent its unit outward normal.

In general, for SE(j_k, $n - ½$), k = 1,2,3, area, unit outward normal, and the spatial coordinates of the centroid of the lateral faces will be referred to as $S^{(l,k)}$, $\hat{n}^{(l,k)} = \left(n_x^{(l,k)}, n_y^{(l,k)}, 0\right)$, and $\left(x_c^{(l,k)}, y_c^{(l,k)}\right)$, l = 1,2. Also the area, and the spatial coordinates of the centroid of the corresponding horizontal plane will be represented by $S^{(k)}$, and

$\left(x_c^{(l,k)}, y_c^{(l,k)}\right)$, respectively. Not that the so-called horizontal planes form the bottom of the octahedron. The horizontal planes that contain the top of the octahedron, however belong to SE(j,n). The area and spatial coordinates of the centroid of the top surfaces are equal to those of the bottom surfaces but their unit outward normal is (0, 0, +1). Using the above conventions and performing the innerproducts, Eq. (49) can be written as

$$\begin{aligned}\int_{S(CE)} \vec{U}\cdot\hat{n}ds = \sum_{k=1}^{3}\Bigg\{ &\int_{S^{(k)}} H(x,y,t;j,n)(+1)ds + \int_{S^{(k)}} H\left(x,y,t;j_k,n-\tfrac{1}{2}\right)(-1)ds \\ &+ \sum_{l=1}^{2}\int_{S^{(l,k)}}\left[F\left(x,y,t;j_k,n-\tfrac{1}{2}\right)n_x^{(l,k)} + G\left(x.y.t;j_k,n-\tfrac{1}{2}\right)n_y^{(l,k)}\right]ds\Bigg\},\end{aligned} \tag{52}$$

where the first and second integrals are performed over the top and bottom surfaces, respectively, and the third integral is related to the lateral faces of the octahedral CE. The third integral in Eq. (52) can be evaluated using Eq. (50) as follows

$$\begin{aligned} I^{(l,k)} = & \int_{S^{(l,k)}}\left[F\left(x,y,t;j_k,n-\tfrac{1}{2}\right)n_x^{(l,k)} + G\left(x.y.t;j_k,n-\tfrac{1}{2}\right)n_y^{(l,k)}\right]ds \\ = & \int_{S^{(l,k)}}\Big\{\Big[F_{j_k}^{n-1/2} + \left(F_x\right)_{j_k}^{n-1/2}\left(x-x_{j_k}'\right) \\ & + \left(F_y\right)_{j_k}^{n-1/2}\left(y-y_{j_k}'\right) + \left(F_t\right)_{j_k}^{n-1/2}\left(t-t^{n-1/2}\right)\Big]n_x^{(l,k)} \\ & + \Big[G_{j_k}^{n-1/2} + \left(G_x\right)_{j_k}^{n-1/2}\left(x-x_{j_k}'\right) + \left(G_y\right)_{j_k}^{n-1/2}\left(y-y_{j_k}'\right) \\ & + \left(G_t\right)_{j_k}^{n-1/2}\left(t-t^{n-1/2}\right)\Big]n_y^{(l,k)}\Big\}ds. \end{aligned} \tag{53}$$

Rearranging leads to

$$
\begin{aligned}
I^{(l,k)} = \int_{S^{(l,k)}} ds \Big\{ & \Big[F_{j_k}^{n-1/2} - \left(F_x\right)_{j_k}^{n-1/2} x_{j_k}' - \left(F_y\right)_{j_k}^{n-1/2} y_{j_k}' - \left(F_t\right)_{j_k}^{n-1/2} t^{n-1/2} \Big] n_x^{(l,k)} \\
& + \Big[G_{j_k}^{n-1/2} - \left(G_x\right)_{j_k}^{n-1/2} x_{j_k}' - \left(G_y\right)_{j_k}^{n-1/2} y_{j_k}' - \left(G_t\right)_{j_k}^{n-1/2} t^{n-1/2} \Big] n_y^{(l,k)} \\
& + \Big[\left(F_x\right)_{j_k}^{n-1/2} n_x^{(l,k)} + \left(G_x\right)_{j_k}^{n-1/2} n_y^{(l,k)} \Big] \int_{S^{(l,k)}} x ds \\
& + \Big[\left(F_y\right)_{j_k}^{n-1/2} n_y^{(l,k)} + \left(G_y\right)_{j_k}^{n-1/2} n_y^{(l,k)} \Big] \int_{S^{(l,k)}} y ds \\
& + \Big[\left(F_t\right)_{j_k}^{n-1/2} n_x^{(l,k)} + \left(G_t\right)_{j_k}^{n-1/2} n_y^{(l,k)} \Big] \int_{S^{(l,k)}} t ds .
\end{aligned}
\tag{54}
$$

But $\int_{S^{(l,k)}} ds$ is the area of the corresponding lateral face and the rest of the above integrals may be evaluated using the space-time coordinates of its centroid. Therefore, the integral becomes

$$
\begin{aligned}
I^{(l,k)} = S^{(l,k)} \Big\{ & \Big[F_{j_k}^{n-1/2} + \left(F_x\right)_{j_k}^{n-1/2} \left(x_c^{(l,k)} - x_{j_k}' \right) + \left(F_y\right)_{j_k}^{n-1/2} \left(y_c^{(l,k)} - y_{j_k}' \right) \\
& + \frac{\Delta t}{4} \left(F_t\right)_{j_k}^{n-1/2} \Big] n_x^{(l,k)} + \Big[G_{j_k}^{n-1/2} + \left(G_x\right)_{j_k}^{n-1/2} \left(x_c^{(l,k)} - x_{j_k}' \right) \\
& + \left(G_y\right)_{j_k}^{n-1/2} \left(y_c^{(l,k)} - y_{j_k}' \right) + \frac{\Delta t}{4} \left(G_t\right)_{j_k}^{n-1/2} \Big] n_y^{(l,k)} \Big\} .
\end{aligned}
\tag{55}
$$

Based on Eq. (50), $I^{(l,k)}$ can also be written as

$$
I^{(l,k)} = \left\{ F\left(x_c^{(l,k)}, y_c^{(l,k)}, t^n - \Delta t/4; j_k, n - 1/2 \right) n_x^{(l,k)} + G\left(x_c^{(l,k)}, y_c^{(l,k)}, t^n - \Delta t/4; j_k, n - 1/2 \right) n_y^{(l,k)} \right\} S^{(l,k)} .
\tag{56}
$$

Following a similar procedure, the first and second integrals of Eq. (52) become

$$
\int_{S^{(k)}} H(x,y,t;j,n)(+1) ds = S^{(k)} \left[H_j^n + \left(H_x\right)_j^n \left(x_c^{(k)} - x_j' \right) + \left(H_y\right)_j^n \left(y_c^{(k)} - y_j' \right) \right]
\tag{57}
$$

and

$$\int_{S^{(k)}} H(x,y,t;j_k,n-1/2)(-1)ds = -S^{(k)}\left[H_{j_k}^{n-1/2} + (H_x)_{j_k}^{n-1/2}\left(x_c^{(k)} - x_{j_k}'\right) + (H_y)_{j_k}^{n-1/2}\left(y_c^{(k)} - y_{j_k}'\right)\right]$$
$$= -S^{(k)} H\left(x_c^{(k)}, y_c^{(k)}, t^{n-1/2}; j_k, n-1/2\right)$$
(58)

respectively. After substitution of the evaluated integrals, provides Eq. (52) an expression for H_j^n. The expression contains three unknowns H_j^n, $(H_x)_j^n$ and $(H_y)_j^n$, but examination of the expressions, which contain $(H_x)_j^n$ and $(H_y)_j^n$ suggest that they may be eliminated, resulting in an explicit method, provided the solution point is selected at the centroid of the hexagon $C_1V_3C_2V_1C_3V_2$ formed by the vertices of cell *j* and the centroids of its three neighbours. Using this, the equation for H_j^n can be written in a convenient manner. Note that despite the apparent complexity, the equation for H_j^n is in fact composed of three similar parts, each related to one of the neighbouring cells.

$$H_j^n = \frac{\sum_{k=1}^{3} R^{(k)}}{\sum_{k=1}^{3} S^{(k)}}, \tag{59}$$

where

$$R^{(k)} = S^{(k)} H\left(x_c^{(k)}, y_c^{(k)} t^{n-1/2}; j_k, n-1/2\right) - \sum_{l=1}^{2} I^{(l,k)} \tag{60}$$

and $I^{(l,k)}$ is evaluated using Eq. (56).

The above formulation has the important attribute of being able to handle non-linearities that may exist in the definition of functions *H*, *F* and *G*. Once the values of enthalpy are updated over the entire domain, Eq. (41) can be used to obtain the temperature field, and the first and second order derivatives of the field parameters may be calculated as described in the following sections.

First order derivatives

Consider Figure 22, where *S*, S_1, S_2 and S_3 are solution points of cell *j* and its three neighbours, respectively, also O_1, O_2 and O_3 denote centroids of triangles SS_2S_3, SS_3S_1, and SS_1S_2, respectively. Using Taylor series (Appendix 4) in triangle SS_2S_3, gives;

$$\begin{aligned} &H_{O_1} + \left(x_j' - x_{O_1}\right)\left(H_x\right)_{O_1}^n + \left(y_j' - y_{O_1}\right)\left(H_y\right)_{O_1}^n = H_j^n \\ &H_{O_1} + \left(x_{j_2}' - x_{O_1}\right)\left(H_x\right)_{O_1}^n + \left(y_{j_2}' - y_{O_1}\right)\left(H_y\right)_{O_1}^n = H, \\ &H_{O_1} + \left(x_{j_3}' - x_{O_1}\right)\left(H_x\right)_{O_1}^n + \left(y_{j_3}' - y_{O_1}\right)\left(H_y\right)_{O_1}^n = H \end{aligned} \tag{61}$$

which after some algebraic manipulations, imply the following equations

$$\left(x_{j_k}' - x_j'\right)\left(H_x\right)_{O_1}^n + \left(y_{j_k}' - y_j'\right)\left(H_y\right)_{O_1}^n = H_{j_k}^n - H_j^n, \tag{62}$$

where $k = 2, 3$. The above system can be solved to give $\left(H_x\right)_{O_1}^n$ and $\left(H_y\right)_{O_1}^n$. A similar procedure can be used in triangles SS_3S_1, and SS_1S_2 to obtain two other systems.

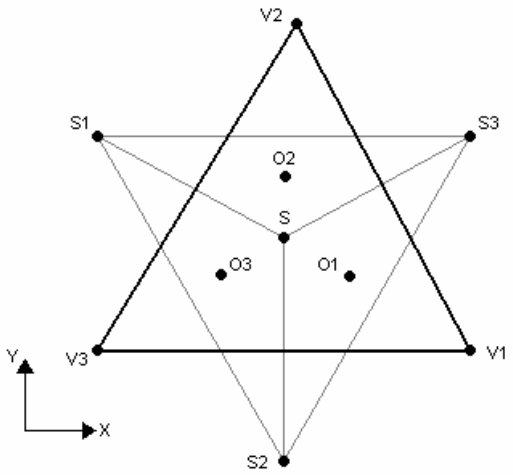

Figure 22. Geometry for calculating first order derivatives.

$$\left(x_{j_k}' - x_j'\right)\left(H_x\right)_{O_2}^n + \left(y_{j_k}' - y_j'\right)\left(H_y\right)_{O_2}^n = H_{j_k}^n - H_j^n, \tag{63}$$

with $k = 1, 3$, and

$$\left(x_{j_k}' - x_j'\right)\left(H_x\right)_{O_3}^n + \left(y_{j_k}' - y_j'\right)\left(H_y\right)_{O_3}^n = H_{j_k}^n - H_j^n, \tag{64}$$

with $k = 1, 2$. These systems can be solved to determine the derivatives at O_2 and O_3. A weighted mean (Appendix 4) may then be used to calculate $\left(H_x\right)_j^n$ and $\left(H_y\right)_j^n$ as follows

$$\left(H_x\right)_j^n = \frac{\sum_{k=1}^{3}\left|\theta_m\theta_p\right|^{\tilde{\alpha}}\left(H_x\right)_{O_k}^n}{\sum_{k=1}^{3}\left|\theta_m\theta_p\right|^{\tilde{\alpha}}}, \left(H_y\right)_j^n = \frac{\sum_{k=1}^{3}\left|\theta_m\theta_p\right|^{\tilde{\alpha}}\left(H_y\right)_{O_k}^n}{\sum_{k=1}^{3}\left|\theta_m\theta_p\right|^{\tilde{\alpha}}}, \tag{65}$$

where

$$\theta_k = \sqrt{\left(\left(H_x\right)_{O_k}^n\right)^2 + \left(\left(H_y\right)_{O_k}^n\right)^2}\,, k = 1, 2, 3 \tag{66}$$

and *kmp* is a non-neutral permutation (Appendix 4) of 1, 2, 3, and the constant α is usually set equal to 1. The above weighted average provides the necessary numerical damping. Note that, to avoid dividing by zero, in practice a small positive number such as 10^{-60} is added to the denominators in Eq. (63). The small technique can be used to calculate the first-order derivatives of temperature. The same values for the first-order derivatives can also be obtained without introducing points O_1, O_2, and O_3 [21].

Second order derivatives

Consider Figure 22, once the first order derivatives of a field parameter (say Ψ) are known, expanding $\left(\Psi_x\right)_{j_k}^{n-½}$, $k = 1, 2, 3$, which is saved at the solution point (S_k, $n - ½$) about the space-time solution point (S, n), the results in three equations.

$$\left(x'_{j_k} - x'_j\right)\left(\Psi_{xx}\right)_j^n + \left(y'_{j_k} - y'_j\right)\left(\Psi_{xy}\right)_j^n - \frac{\Delta t}{2}\left(\Psi_{xt}\right)_j^n = \left(\Psi_x\right)_j^{n-½} - \left(\Psi_x\right)_j^n, \quad k = 1,2,3. \tag{67}$$

These may be solved simultaneously for $\left(\Psi_{xx}\right)_j^n$, $\left(\Psi_{xy}\right)_j^n$, and $\left(\Psi_{xt}\right)_j^n$. A similar system gives $\left(\Psi_{yx}\right)_j^n$, $\left(\Psi_{yy}\right)_j^n$, and $\left(\Psi_{yt}\right)_j^n$. Using this technique, the mesh values of second-order derivatives of T can be evaluated in order to be used in Eq. (51). The first-order derivatives of flux functions, evaluated from Eq. (51), can then be used in Eq. (59).

Boundary conditions

In order to treat the boundary conditions, a ghost cell is defined for each boundary cell, see Figure 23.

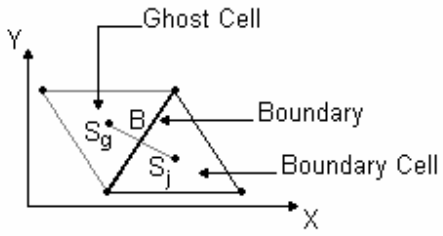

Figure 23. Boundary and ghost cells.

Geometrically, the ghost cell is a mirror image of the corresponding boundary cell with respect to the boundary, as shown in Figure 23, where S_j and S_g denote solution points related to the boundary cell and the ghost cell, respectively, and B is the intersection of the line S_g and S_j with the boundary.

Let Ψ be a field parameter, which can be either enthalpy or temperature.

1. Constant temperature boundary Ψ_B = constant:
   Using linear interpolation $\Psi_g = 2\Psi_B - \Psi_j$; all derivatives at ”*g*” may then be set equal to their corresponding values at ”*j*”.

2. Reflecting boundary condition; the insulated boundary, axis of symmetry:
   Let σ and τ be the normal and tangential directions to the boundary, respectively.

The insulation condition is then

$$\left(\frac{\partial T}{\partial \sigma}\right)_{\text{boundary}} = 0 \tag{68}$$

and considering

$$\frac{\partial H}{\partial \sigma} = c\frac{\partial T}{\partial \sigma} \tag{69}$$

it also leads to

$$\left(\frac{\partial H}{\partial \sigma}\right)_{\text{boundary}} = 0\,. \tag{70}$$

7.3 Homogenization

The theory of homogenization can describe the behavior of composite materials. Composite materials contain two or more finely mixed constituents. They have in general better properties than the properties of their individual constituents and play an important role in many branches of Mechanics, Physics, Chemistry and Engineering. Typically, in such materials, the physical parameters (conductivity, elasticity coefficients, etc.) are discontinuous and oscillate between the different values characterizing each of the components. Two scales are used to understand and describe the general behavior of the composite, the microscopic and the macroscopic. The aim of homogenization is to give the macroscopic properties of the composite by taking into account the properties of the microscopic structure. After the problem has been homogenized the oscillating

coefficients has been replaced with constant coefficients, which made the partial differential equation well suited for being solved numerically [11]. In scrap melting the microscopic and macroscopic behavior can be the scrap and the air in the furnace. This works as a porous media.

As a model case[5] [11]; consider a homogeneous body occupying Ω with thermal conductivity γ. I *f* represent the heat source, *ρc*, material-constant, and *g* the temperature on the surface $\partial\Omega$ of the body, then the temperature $u(x,t)$ at the point $x \in \Omega$ satisfies the following Dirichlet problem.

$$\begin{cases} \rho c \dfrac{\partial u}{\partial t} - div\big(\gamma(x) Du(x,t)\big) = f(x,t) & \text{in} \quad \Omega \\ u = g & \text{on} \quad \partial\Omega \end{cases}, \tag{71}$$

where *Du* denotes the gradient of *u*.

$$Du = \text{grad } u = \left(\frac{\partial u}{\partial x_1}, \ldots, \frac{\partial u}{\partial x_n} \right). \tag{72}$$

For simplicity the material is assumed to be isotropic[6], that is γ is a scalar, and $g(x) = 0$, which obtain

$$\begin{cases} -\gamma \Delta u = f & \text{in} \quad \Omega, \\ \text{u} = 0 & \text{on} \quad \partial\Omega, \end{cases} \tag{73}$$

[5] The model case includes functional analysis, which is further explained in [11]
[6] Isotropic means having identical properties in all directions.

where Δu = div (Du). The flux of the temperature is defined by

$$q = \gamma Du \,. \tag{74}$$

This is a classical elliptic boundary value problem and if f is sufficiently smooth, it admits a unique solution u, which is twice differentiable and solves system (73) at any point x in Ω. In a heterogeneous material, γ is not a scalar, that is $\gamma = \gamma(x)$. For example in material with two different constituents, the thermal conductivity takes different values in each component of the composite and thus γ is discontinuous in Ω.

Consider a body containing two constituents, one occupying Ω_1 and the second Ω_2, with $\Omega_1 \bigcap \Omega_2 = \emptyset$, and $\Omega = \Omega_1 \bigcup \Omega_2 \bigcup (\partial\Omega_1 \bigcap \partial\Omega_2)$. Suppose that the thermal conductivity of the body occupying Ω_1 is $\gamma_1(x)$ and that of the body occupying Ω_2 is $\gamma_2(x)$, Figure 24. The thermal conductivity is discontinuous in Ω, since it jumps over surfaces, which separate the constituents.

$$\gamma(x) = \begin{cases} \gamma_1(x) & \text{if} \quad x \in \Omega_1 \\ \gamma_2(x) & \text{if} \quad x \in \Omega_2 \end{cases} \quad . \tag{75}$$

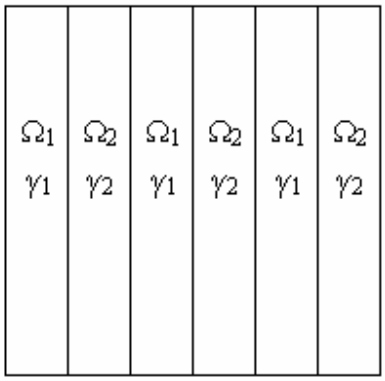

Figure 24. The thermal conductivity of the body occupying Ω_1 is γ_1 and of the body occupying Ω_2 is γ_2.

Then the temperature and the flux of the temperature in a point $x \in \Omega$ of the composite respectively take the values;

$$u(x) = \begin{cases} u_1(x) & \text{if} \quad x \in \Omega_1 \\ u_2(x) & \text{if} \quad x \in \Omega_2 \end{cases} \tag{76}$$

and

$$q = \begin{cases} q_1 = \gamma_1 Du_1 & \text{in} \quad \Omega_1 \\ q_2 = \gamma_2 Du_2 & \text{in} \quad \Omega_2 \end{cases}. \tag{77}$$

The corresponding system to (71) now reads

$$\begin{cases} -div\big(\gamma(x)Du(x)\big) = f(x) & \text{in} \quad \Omega_1 \bigcup \Omega_2, \\ u = 0 & \text{on} \quad \partial\Omega, \\ u_1 = u_2 & \text{on} \quad \partial\Omega_1 \bigcap \partial\Omega_2, \\ q_1 \cdot n_1 = q_2 \cdot n_2, & on \quad \partial\Omega_1 \bigcap \partial\Omega_2, \end{cases} \tag{78}$$

n_i is the outward normal unit vector to $\partial\Omega$ for I = 1, 2 and $n_1 = -n_2$. Thus the system (78), it follows that the gradient of u is discontinuous, and in general the flux $q(x) = \gamma Du$ is not differentiable. Hence one can not expect solutions of class C^1. The question is in which function space can there be a solution. The weak formulation (Appendix 4) of (78) is;

$$\begin{cases} -div\big(\gamma(x)Du(x)\big) = f(x) & \text{in} \quad \Omega \\ u \in H, \end{cases}, \tag{79}$$

where H is an appropriate Sobolev space taking into account the boundary conditions on u. The derivatives are taken in the sense of distributions. Not that (79) should be considered as

$$\begin{cases} \text{find } u \in H \text{ such that} \\ \int_\Omega \gamma(x) \dfrac{\partial u}{\partial x_i} \dfrac{\partial v}{\partial x_i} dx = \int_\Omega fv dx, \quad \forall v \in H. \end{cases} \tag{80}$$

If u were sufficiently smooth, (78) and (79) would be equivalent. But this is not the case for a composite material. Suppose that the heterogeneities are very small with respect to the size of Ω and that they are evenly distributed. This is a realistic assumption for a large class of applications. As a simplification, it is assumed that the distribution can be modeled as a periodic one, se Figure 25. This periodicity can be represented by a small parameter ε. Then γ in (80) depends on ε and (80) reads;

$$\begin{cases} \text{find } u^{\varepsilon} \in H \text{ such that} \\ \int_{\Omega} \gamma^{\varepsilon}(x) \dfrac{\partial u^{\varepsilon}}{\partial x_i} \dfrac{\partial v}{\partial x_i} dx = \int_{\Omega} fv dx, \quad \forall v \in H. \end{cases} \tag{81}$$

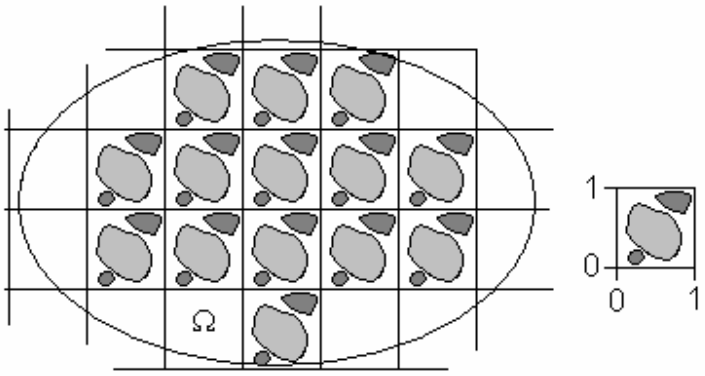

Figure 25. Periodic structure of Ω and the Y-cell.

In mathematical model of microscopically heterogeneous materials, various local characteristics are usually described by maps of the form $a^{\varepsilon}(x) = a\left(\dfrac{x}{\varepsilon}\right)$. A natural way to introduce the periodicity of γ^{ε} is (81) is to suppose that it has the form;

$$\gamma^{\varepsilon}(x) = \gamma\left(\frac{x}{\varepsilon}\right) \text{ a.e. on } \mathrm{R}^{\mathrm{n}}, \tag{82}$$

where γ is a given periodic function of period *Y*. This means that a reference period *Y*, in which the reference heterogeneities are given. By definition (82), the heterogeneities in Ω are periodic of period εY and their size is of order ε. Problem (81) is then written as follows;

$$\begin{cases} \text{find } u^{\varepsilon} \in H \text{ such that} \\ \int_{\Omega} \gamma\left(\dfrac{x}{\varepsilon}\right) \dfrac{\partial u^{\varepsilon}}{\partial x_i} \dfrac{\partial v}{\partial x_i} dx = \int_{\Omega} fv dx, \quad \forall v \in H. \end{cases} \tag{83}$$

An example of periodic structure of Ω is shown in Figure 25. Observe that two scales characterize our model problem (83), the macroscopic scale *x* and the microscopic scale

$\frac{x}{\varepsilon}$, describing the micro-oscillations. Also observe that making the heterogeneities smaller and smaller means that the mixture is being homogenize and from the mathematical point of view this means that ε tends to zero. Taking $\varepsilon \to 0$ is the mathematical homogenization of problem (83).

Homogenization theory is the aim of answering the questions [11];

1. Does the function u^{ε} converge to some limit function u^0?
2. If that is true, does u^0 solve some limit boundary value problem?
3. Are the coefficients of the limit problem constant?
4. Finally, is u^0 a good approximation of u^{ε}?

The problem of flow through a porous medium may be treated by the homogenization method, but only for a periodic model of such a medium.

8 The physical model

The model will simulate how scrap steel is melted in an electric arc furnace. The aim is to investigate how steel scrap is melted in a one electrode DC furnace.

The melting process is an effect of the heat from the arc and the convective heat transfer in the liquid metal. This means that the scrap is of various shapes. The heat and mass transfer between liquid and solid phases is a complex problem. As soon as the melting begins the molten liquid drips down toward the bottom of the furnace. Thereafter, the liquid level rises while the height of the scrap metal decreases. The scrap is heated both from the arc and the liquid at the bottom, Figure 26.

A wise man said; “All models are wrong, but some of them are useful”. In the normal world there is no constant place were anyone could simulate all that is in an EAF, except in an EAF. And even then there are many variables that can change. The purpose is to use a hot air gun to melt ice, as a simulation as the arc melts the scrap. Magnetic fields are neglected.

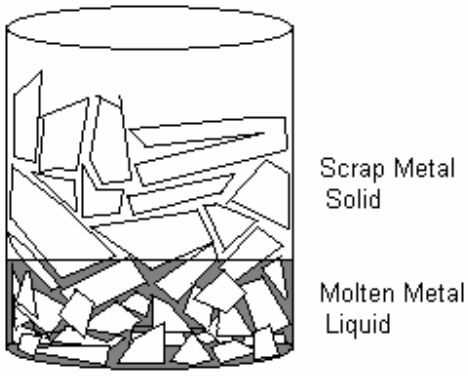

Figure 26. At the top there are only solids, and at the bottom there are solids melting in liquid.

To simplify the testing ice is used instead of steel scrap. The reasons to use ice are for example that it is easy to find, work with and can easily model the scrap. For example the specific heat capacity is about 460 J/kgK for steel and 419 J/kgK for water [29]. However thermal conductivity for water is 0.60 W/mK and for steel 45 W/mK [29], this is neglected in the physical model, since the conducting ability is not the primary melting mechanism in the EAF [23].

The hot air gun simulates the heat from the arc. The model gives data on how fast the ice is melting during a specific time and a specific air-stream temperature. Measurements with various changes, in air flow, amount of ice, “arc length” etc. will give results that later can be used in a CFD model.

Each experiment takes approximately 10-20 min. The measurements have been done, with different:

- air flows, the volume of air from the hot air gun, 150-500l/min
- temperature of the air flow from the hot air gun, 50-630^{o}C
- distance between the hot air gun and the ice
- amount of ice, maximum weight of scales is 5 kg
- shapes of ice-blocks, Squares, crushed etc.
- bowls.

First thing to do was to investigate a “good” distance, between the ice and the hot air gun with fixed setting on the hot air gun. After investigating different types of ices, change in other parts of the above was done. It is interesting how the temperature changes when the ice melts. The experiments was filmed, so that further investigations can be made.

8.1 Building the model

The building of the melting model started with a test model to understand the equipment. The PR electronics Universal Transmitter 4116 is used together with a Mettler Toledo scale and two thermal elements, Figure 27.

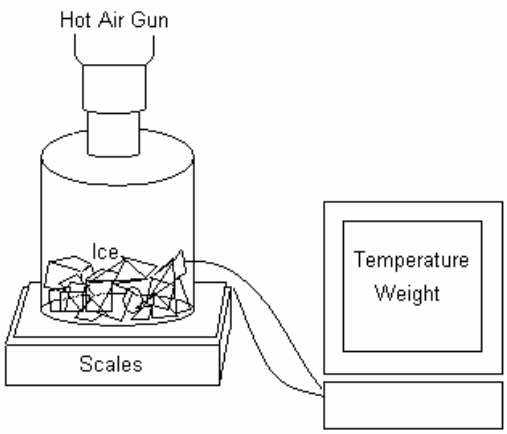

Figure 27. A simple melting model, to measure temperature changes over time.

The first model also detected the weight, but in this case the weight is not as interesting, since it should not vary that much, see Figure 28. This model worked in some way, but

did not provide good results, since it could not show the weight changes as the ice turns to water.

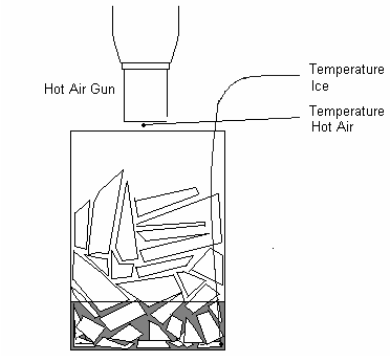

Figure 28. The first model used to melt the ice.

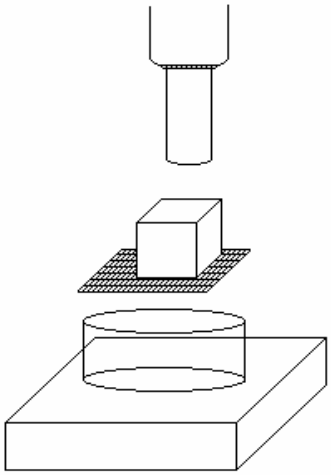

Figure 29. The second model of melting used a net and weighted only the water.

In the second model a net is used, so that only the molten ice was weighted, i.e. the water, see Figure 29. The problem was that the amount of ice needed for better results sometimes slid of the net. This gave two options, either a bigger model or a pipe, so that the ice can't slide of the net, and the environmental influence will be less.

The third model used a net inside a pipe, the kind of pipes used for ventilation, see Figure 30 and Figure 31. The pipe is 100 mm in diameter. Now the melting curves is viewed. However there are still some losses when the ice is melted. Losses were expected, but the losses vary and were still quite big, which can not be ignored.

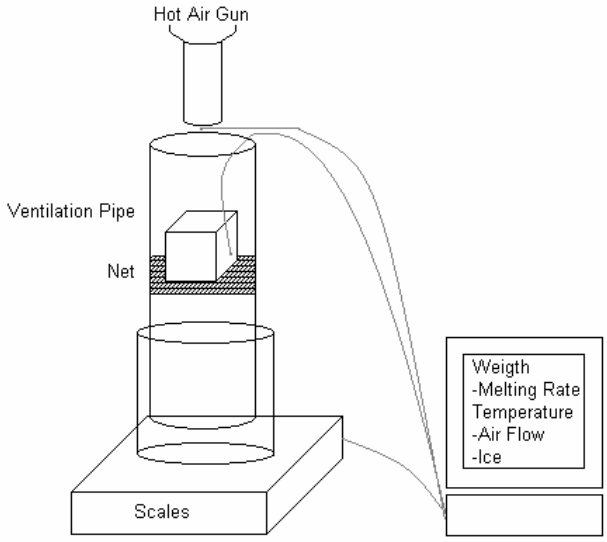

Figure 30. The third model of melting was made inside a ventilation pipe.

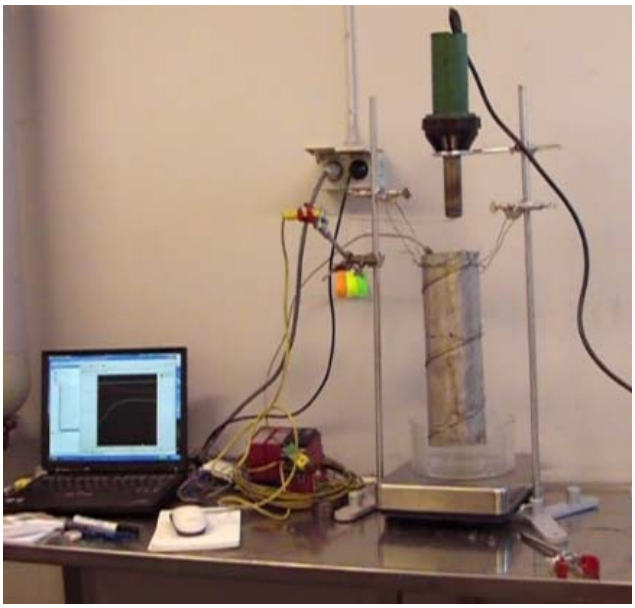

Figure 31. The ventilation pipe model.

The last model is made of acrylic glass, also called Plexiglas. The temperature is measured at the bottom of the bucket see Figure 32 and Figure 33. This gives varying temperature measurements of the ice. The air stream does not affect the scales, which gives smoother weight curves. There is practically no losses or gains when the ice turns into water.

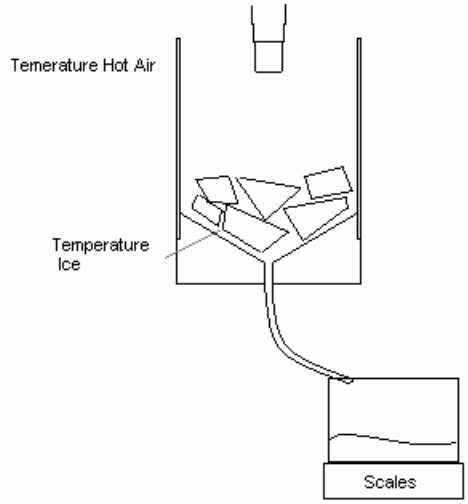

Figure 32. The forth model made of Acrylic glass.

Figure 33. The Acrylic glass model uses a hose to lead the water to the bowl on the scales.

The bottom of the cylinder is made of a plastic piece that is curved with a drip-angle, v that is 60^{o}, see Figure 34 . The diameter of the cylinder is 170 mm, and the thickness of the acrylic glass is 4 mm.

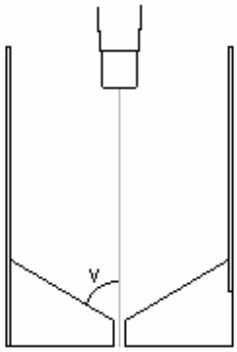

Figure 34. The drip angle, v in the acrylic glass model.

More pictures of this model can be seen in Appendix 3. The melting curves are smooth when logging the weight of the melted water – time. The weight of the molten can fits a polynomial equation, as shown in chapter 8.2.

8.2 Results and discussion

8.2.1 Air flow

The model is measuring temperature of the air flow, from two types of hot air guns, the Steinel HL2010 E and a Leister hot air gun used to weld carpets. The temperature is not steady with the Steinel hot air gun, since the hot air gun gets overheated, see Figure 35. The degrees that can be set on the Steinel hot air gun is not the same as the hot air coming out of the mouthpiece. This means that its temperature element is inside the hot air gun. The temperature setting is continuous in 10^{o}C steps by pushbutton controls and is displayed on a LCD display. The Leister hot air gun is used to weld carpets together. It has the temperature sets in a scale of 1-10, the temperature is measured in the model, see Figure 36.

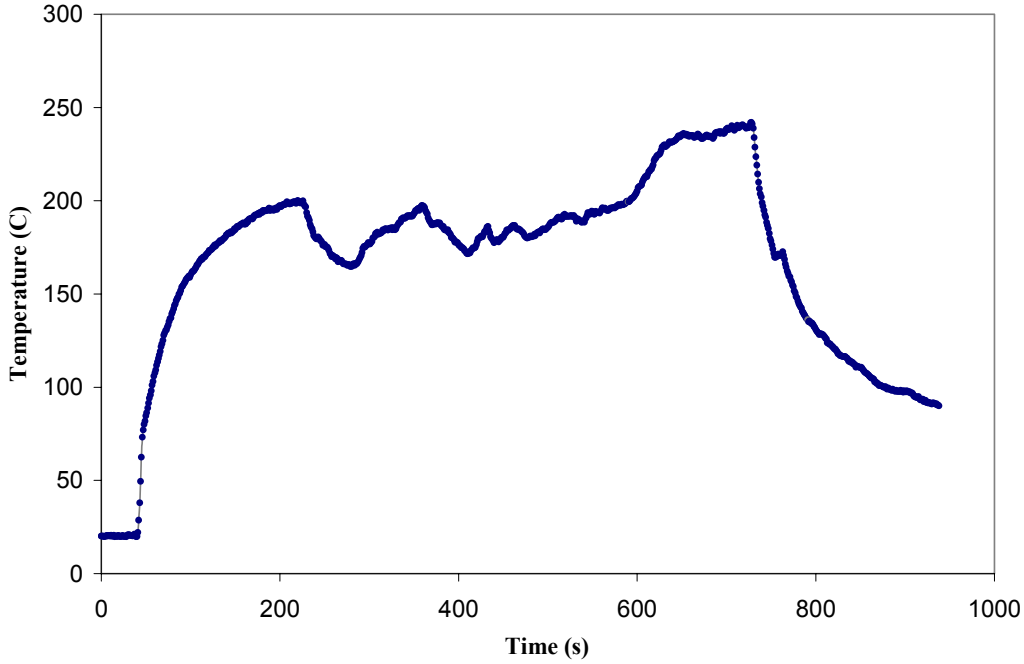

Figure 35. Temperature of the air flow, with a Steinel HL20140E at II, 400°C.

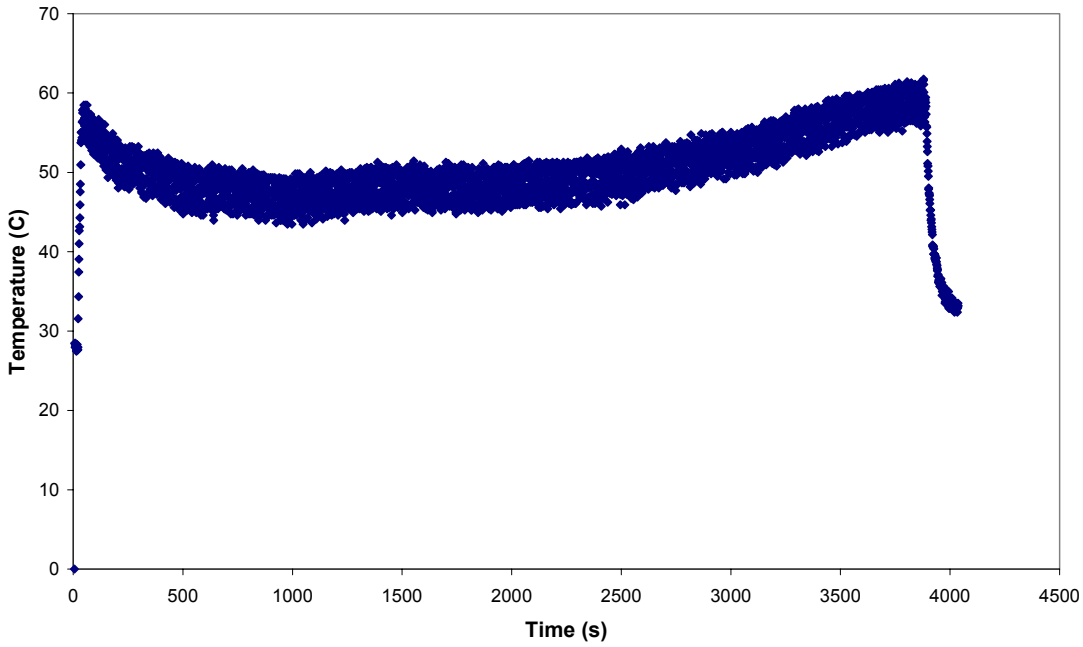

Figure 36. Leister hot air gun gives smother temperature curves.

$\dot{V}$ is the volume flow of hot air (m^3/s), v is the speed of the hot air and A is the area of the nozzle.

$$\dot{V} = v \cdot A \Leftrightarrow v = \frac{\dot{V}}{A} \tag{84}$$

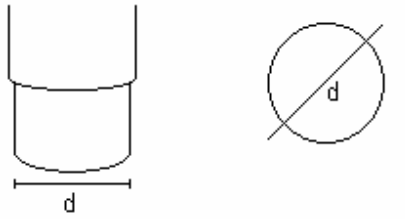

Figure 37. Diameter of the nozzle.

d = Diameter of the nozzle, see Figure 37.

This gives for the Leister hot air gun the following equations; volume flow $\dot{V} = \max 230$ l/min, according the instruction manual and d = 15 mm, which gives $v_{max} \approx 21{,}7$ m/s.

The Steinel HL2010 E has three different regulations of the flow, and the temperature can be regulated in steps of 10°C, from 50 to 600°C. The instruction manual gives the volume flow $\dot{V} = 150$, 300 and 500 l/min for I, II and III respectively. The diameter of the nozzle is measured to d = 22mm, which gives $v_I \approx 6{,}6$ m/s, $v_{II} \approx 13{,}2$ m/s and $v_{III} \approx 21{,}9$ m/s respectively.

8.2.2 Melting time comparison

30 ice cubes are melted to compare the melting times. Natural convection means that the ice is melting without any tool except the room temperature, 24°C. It is clear that the water is melting the still left ice, see Figure 38. The time to melt the ice, without air flow, when the molten liquid is transported to a scale, where it is measured is for 30 ice cubes approximately 10 h 15 min. If the molten water is left the melting time is approximately 6 h 21min.

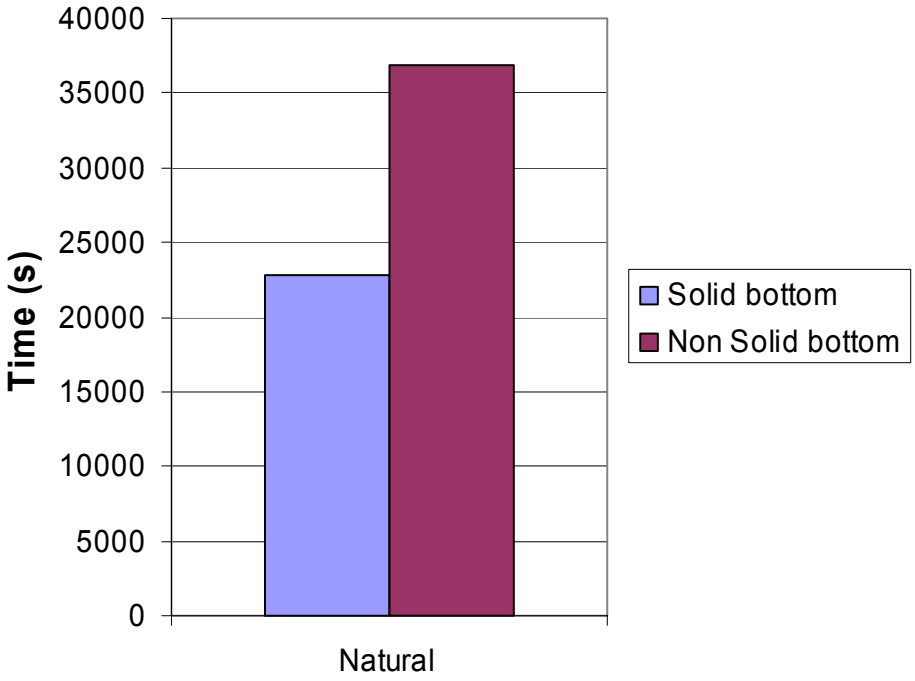

Figure 38. Time to melt the 30 ice cubes, with only natural convection is compared.

Figure 39. Melting comparison when a Hot Air Gun is used.

Melting time measured with forced convection from a hot air gun gives; 7 min 24 s to melt ice without a hole, using the Leister hot air gun set at 10, the same experiment with a hole, where the molten liquid is dripped down away from the melting area takes 6 min 40 s. It is to be noted that the time to melt 30 ice cubes is over 90 times faster with a hot air flow from the Leister hot air gun than with only the surroundings. If the Leister hot air gun is set to 5, or the Steinel HL2010 E, II 200^{o}C is used, the results in melting time, is 16 min 13 s, and 21 min 9 s respectively. See Figure 38 and Figure 39.

This means that the forced convection from the hot air gun melts the ice faster than the natural convection of the molten liquid. This in this case the water probably is cooling the ice from below, while the hot air is blocked by the ice floating on the surface.

8.2.3 Differences between the EAF and the water/ice model

The difference between melting ice in this model and melting steel in a DC furnace.

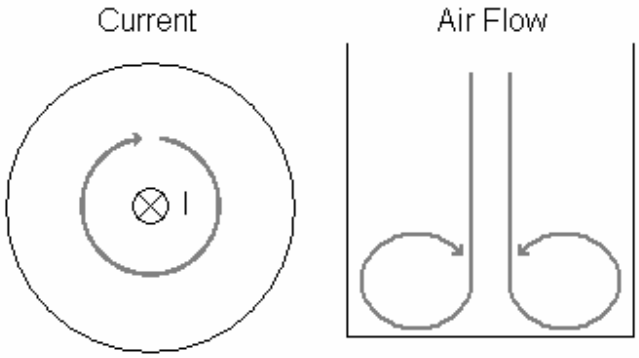

Figure 40. The current give a magnetic field, which give some stirring, while the air flow give turbulence at the bottom of the furnace.

The current in a DC furnace give a magnetic field, which give some stirring. The air flow gives turbulence at the bottom of the furnace. This means that is very different field in the hot air model contra a DC furnace, Figure 40.

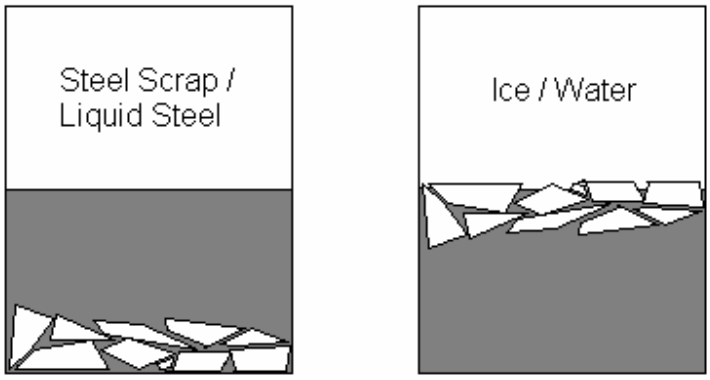

Figure 41. The solid steel draws down in the melt as compared to ice, which is on top of water.

Liquid steel has lower density then solid steel, which means that when the steel melts the solids is at the bottom of the furnace, which gives larger amount of convection through the melt, but significantly smaller radiation heat from the plasma. In an ice/water model the ice has lower density then water, which means that the ice floats, see Figure 41. This gives that the melting from radiation, or in this case forced convection as well as the natural convection from the melt melts the ice.

Heat losses through the acrylic glass, is measured with stationary conduction [27];

$$\dot{Q} = \frac{2\pi k l (T_1 - T_2)}{\ln\left(\frac{r_2}{r_1}\right)}, \tag{85}$$

where T_1 and T_2 are inner and outer temperature and r_1 and r_2 are inner and outer radius (see Figure 42), and l is the length of the acrylic glass pipe and k is thermal conductivity; k = 0.2 W/m·K for acrylic glass. The bottom and the surface of the physical model are assumed to be adiabatic.

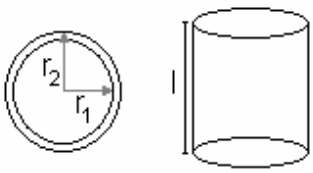

Figure 42. Inner and outer radius and length of the acrylic glass pipe, to predict heat losses.

8.2.4 Comparison results

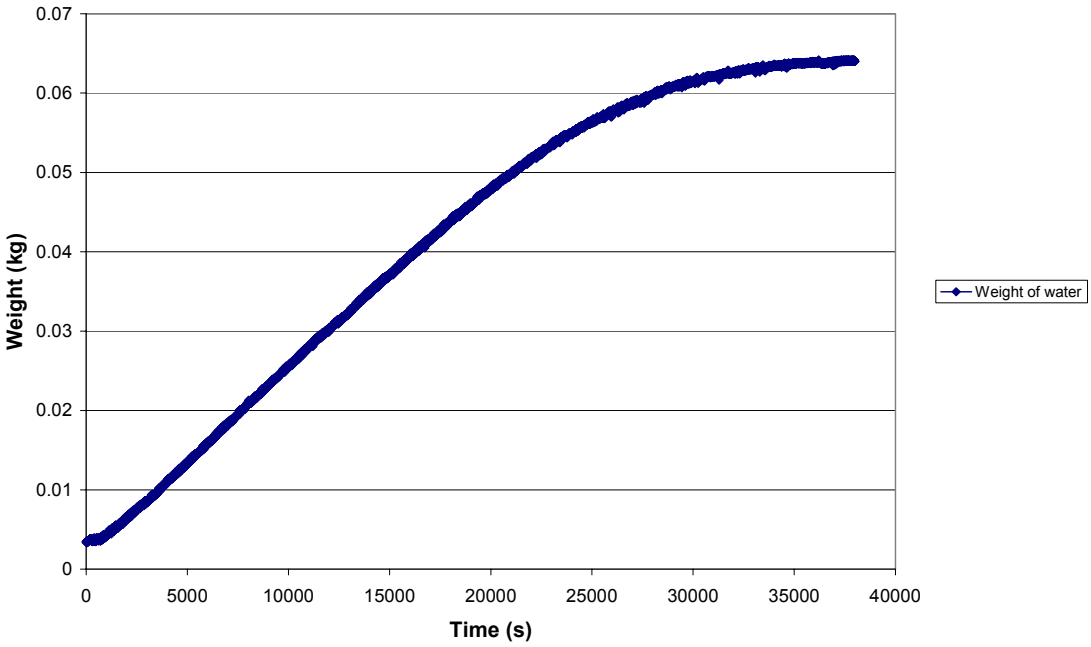

Figure 43. Melting Rate without air flow, molten liquid is measured, 30IC is used.

A trendline on the melting rate curve gives a smooth fourth polynomial function, where y represents the weight of the molten ice, i.e. the water and t is the time, see Figure 43 ;

$$y = 4 \cdot 10^{-17} \cdot t^4 - 2 \cdot 10^{-12} \cdot t^3 + 3 \cdot 10^{-8} \cdot t^2 + 0.0004 \cdot t + 0.2629 \quad (86)$$

with

$R^2 = 0.9999$.

More about R^2 is in appendix 4. Compare with measurement melting rate where the leister hot air gun is used, see Figure 44 . This gives another fourth polynomial trendline, since the melting time is different, compare with Figure 39;

$$y = 8 \cdot 10^{-10} \cdot t^4 - 9 \cdot 10^{-7} \cdot t^3 + 0.0003 \cdot t^2 - 0.0172 \cdot t + 0.4762 \quad (87)$$

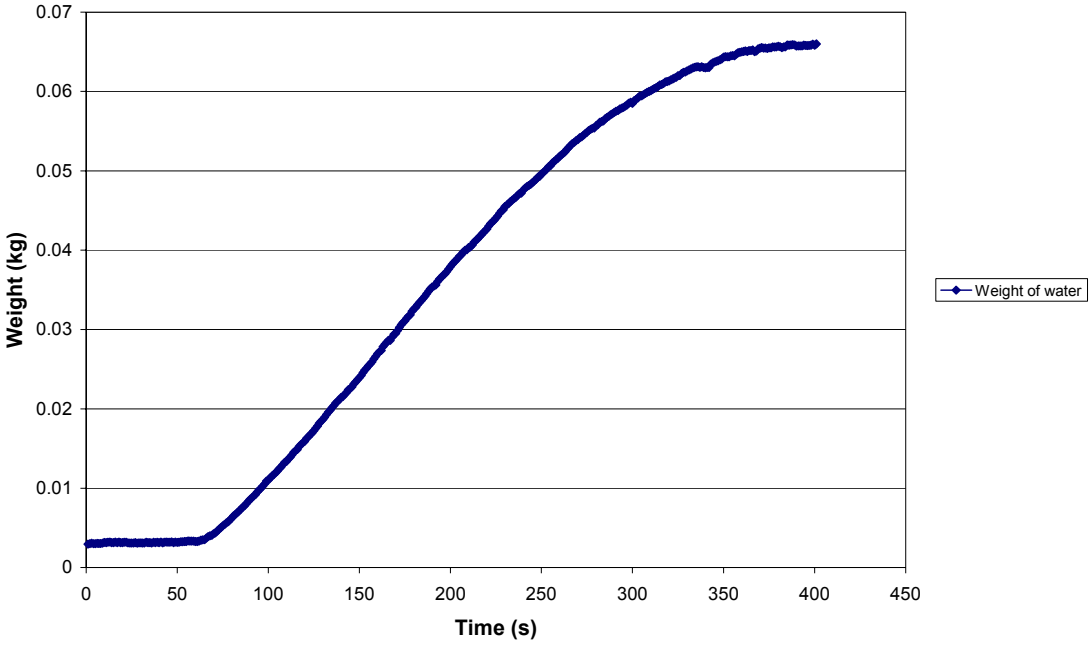

Figure 44. Melting Rate with and Leister air flow 10, molten liquid from 30 ice cubes is measured.

9 Future developments and conclusions

The physical model is built and that was the bigger part of the project. The results from the measurements will be used as input in simulations using CFD in order to make a numerical model of melting in an EAF. It would be interesting if homogenization method and for example CE/SE methods could be combined, in the CFD model. In that case there would both an analytical and numerical solution, to compare.

The physical model can also be used to melt metals with low melting points, for example tin. This measurement will give comparison result to the water trials, and can be used to understand the problem with the conduction ability in the steel contra other metal or water.

10 References

[1] Kawakami M, Takatani K, Brabie L (1999) *Heat and mass transfer analysis of scrap melting in steel bath*, Tetsu-To-Hagane/ Journal of the Iron and Steel Institute of Japan, v 85, n 9, Sep, 1999, p 658-665, ISSN: 0021-1575.

[2] Li J., Brooks G., Provatas N. (2004) *Phase-Field Modeling of Steel Scrap Melting in a Liquid Steel Bath*, AISTech 2004 Proceedings, Volume I, p 833-843.

[3] Li J., Brooks G., Provatas N. (2004) *Kinetics of Scrap Melting in Liquid Steel*, Metallurgical and materials transactions B, Volume 36B, April 2005, p 293-302.

[4] Wu Y, Lacroix M (1993) *Numerical Study of Melting of Scrap Metal*, Canada, Numerical Heat Transfer, Part A, vol. 24, pp.413-425, 1993.

[5] Wu Y, Lacroix M (1995) *Numerical simulation of the Melting of Scrap Metal in a circular furnace*, Canada, Int. Comm. Heat ass Transfer, Vol. 22, No. 4.pp. 517-525, 1995.

[6] Wu Y. *et al* (1993) *A heat transfer model for the melting of aluminum scrap*. Light Metals 1993, The Minerals, Metals & Material Society, 1992

[7] Chang S.C., Wang X.Y., Chow C.Y. (1998) *The Space-Time Conservation Element and Solution Element method –A New High-Resolution and Genuinely Multidimensional Paradigm for solving Conservation Laws.* [online] Nasa, USA. Available: http://ntrs.nasa.gov/archive/nasa/casi.ntrs.nasa.gov/19990019484_1999011466.pdf [2006, June 2]

[8] Ayasoufi A., Keith T.G. (2002) *Application of the conservation element and solution element method in numerical modeling of heat conduction with melting and/or freezing*, International Journal of Numerical Methods for Heat & Fluid Flow Vol. 13 No.4, 2003 pp 448-472.

[9] Ayasoufi A., Keith T.G. (2004) *Application of the Conservation Element and Solution Element Method in Numerical Modeling of Axisymmetric Heat Conduction with Melting and/or Freezing*, JSME international Journal Series B, Vol. 47, No.1, 2004.

[10] Ayasoufi A., Keith T.G., Rahmani R.K. (2004) *Application of the Conservation Element and Solution Element Method in Numerical Modeling of Three-Dimensional Heat Conduction with Melting and/or Freezing*, Journal of Heat Transfer, December 2004, Vol. 126, p 937-945

[11] Dasht J. (2001) *Homogenization of some Partial Differential operators*, Master Thesis, Luleå: Dept. of Math. Luleå University of Technology, Luleå Sweden.

[12] Jernkontoret, Sweden. [online]. Available: http://www.jernkontoret.se [2006, May 17].

[13] Luleå Tekniska Universitet. *Huvudkurs i Processmetallurgi, Kurslitteratur i KMP017– Stålframställning och efterbehandling av stål*, Sammanställt 2001, Luleå Tekniska universitet, institutionen för Kemiteknik, Luleå 2001.

[14] Höganäs AB, Sweden. [online]. Available: http://www.hoganas.com [2006, May 17].

[15] Glossary of materials science. [online]. Matter. Available: http://www.matter.org.uk/glossary [2006, May 17].

[16] Stena Gotthard AB, Sweden. [online]. Available: http://www.stenagotthard.com [2006, May 17].

[17] Svenska Metallkretsen AB, Sweden. [online]. Availabe: http://www.metallkretsen.se [2006, May 17].

[18] Bonnier M, *Konservburkar - ett miljöproblem?* Projektarbete i kursen Miljövård, Översiktskurs, 5 poäng, ht 1997, Lund 1997-1998, Sweden. [online]. Available: http://www.df.lth.se/~mikaelb/environ/cans-sve.shtml [2006, May 17].

[19] Erasteel Kloster AB *et al* (2005) *Skrotboken 2000 utgåva 1, Bestämmelser för leverans och klassificering av stålskrot och gjutjärnsskrot*, Sweden.

[20] Lankford Jr WT, *et al* (1985) *The Making, Shaping and Treating of Steel*. 10th edition, United States Steel, Pittsburgh, Pennsylvania U.S.A. ISBN 0-930767-00-4.

[21] Mefos – Metallurgical Research Institute AB. [online] Available: http://www.mefos.se [2006, May 17]

[22] Ångström, Sten (1998) *Utbildningskompendium Elektrisk smältning och värmning av stål*. Tekniskt Meddelande, Mefos – Metallurgical Research Institute, Luleå Sweden. TM98041.

[23] Alexis J. *et al* (2000) *Modeling of a DC Electric Arc Furnace – Heat Transfer from the Arc*, ISIJ International, November 2000, Vol.40, No. 11, p 1089-1097.

[24] Svensson P (2001) *Induktiv omrörare till ljusbågsugn*, Examensarbete, Luleå, Sweden: Luleå Tekniska Universitet 2001:348. ISSN: 1402-1617. ISRN: LTU – EX – 01/348 – – SE.

[25] Alexander C.K., Sadiku M.N.O (2000) *Fundamentals of Electric Circuits*. USA: McGraw-Hill Higher Education ISBN 0-256-25379-X.

[26] Incropera Frank P, De Witt David P.(2002) *Introduction to Heat Transfer* 4th edition New York, USA: John Wiley & Sons. ISBN 0-471-38649-9.

[27] Henja T, Fällström K-E, Hermansson R (1996) *Grundläggande värmeöverföring*. Luleå, Sweden: Tekniska Högskolan i Luleå.

[28] Bejan A, Kraus A, (2003) *Heat Transfer Handbook*, John Wiley & Sons, ISBN 0-471-39015-1, Electronic ISBN 1-59124-513-3. [online]. Knovel Library. Available: http://www.knovel.com

[29] Nordling C., Österman J. (2004) *Physics Handbook for Science and Engineering*, Seventh edition Lund, Sweden: Studentlitteratur ISBN 91-44-03152-1.

[30] cfd-online. [online] Available: http://www.cfd-online.com [2006, May 17].

[31] wikipedia. [online] Available: http://www.wikipedia.org [2006, May 17].

[32] Råde L, Westergren B. (1998) *Mathematics Handbook for Science and Engineering*, Fourth edition Lund, Sweden: Studentlitteratur ISBN 91-44-00839-2.

Appendix

Appendix 1

Classification of steel scrap

From Skrotboken 2000:1, [19], where guiding principles for the steelworks technical purchase specifications and the scrap-trades manufacturing directions publishes. Examples of classification of steel scrap in Table 2.

Table 2. Example on classification of steel scrap [19].

Klass/class	Benämning	Designation
101	Prima styckeskrot	First-rate scrap piece
117	Fragmenterat skrot	Fragmentised scrap
12	Sekunda Styckeskrot	Second-rate scrap piece
21	Spånskrot	Chip scrap
31	Prima lost tunnplåtskrot	First-rate loose sheet metal scrap
32	Prima pressat tunnplåtskort	First-rate pressed sheet metal scrap
37T	Fragmenterade eller pressade konserburkar	Fragmentised or pressed tins
622	Kopparlegerat styckeskrot	Copper alloyed scrap piece

Cast iron scraps is classified in a similar way, but are divided in fewer classes of scrap, Table 3 [19]:

Table 3. Classification of cast iron scrap [19].

Klass/ class	Benämning	Designation
711	Prima Styckeskrot	First-rate scrap piece
721	Sekunda Styckeskrot	Second-rate scrap piece
741	Spånskrot	Chipscrap
742	Spånskrot Briketterat	Chipscrap Briquetted

For example class 101-First-rate scrap piece, is classified in this way [19]:

Description: unalloyed steel scrap, free of bulky, hollow, scrap that is hard to handle and must rusted scrap. Protection paint can be included.

Thickness: At least 6 mm.

Volume-mass: At least 0,7 ton/m^3.

Format: At most 1500x500x500 mm, 1000x800x500 mm or 500xdiameter 600mm. Piece weight at most 1000kg.

Observe: In this class does not include:

a) Chromium-plated, nickel-plated or zinc-plated scrap.
b) Reinforcement iron

Explanations: With bulky, hollow material means such material with the volume according to weight is large, from example pipes with larger inner-diameter than 250 mm. Scarp that considers hard to handle is scrubby, barrier and coherent scrap.

Appendix 2

Nomenclature

P, p	Power (W)
U, u	Voltage (V)
I, i	Current (A)
R	Resistance (Ω)
E	Energy (J)
t	Time (s)
f	Frequency (Hz)
X	Reactance
Z	Impedance
η	Efficiency
T	Temperature
$\dot{q}$	Heat flux
λ	Wavelength
c	Speed of light in empty space; $2.997\ 924\ 58 \cdot 10^8$ m/s
K, k_s, k_l, γ	Thermal conductivity
P	Mass density
C_p, c	Specific heat
H	Heat transfer coefficient
L_f	Latent heat of fusion
v	Moving velocity of the interface (melting rate)
δ	Porosity
H, h	Total, sensible enthalpy
f_l	Local liquid fraction
$\widetilde{S}, q$	Heat source term
β	Flame blocking factor
γ	Flame damping factor
F, G	Flux functions
Ψ	Field parameter

Appendix 3

Photos of the measurement equipment

Figure A1. Acrylic glass model, with Steinel hot air gun.

Figure A2. The ice is filled in the model, which has a hole in the bottom.

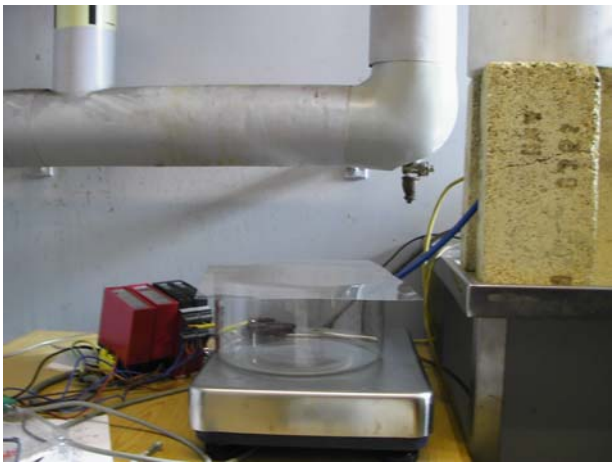

Figure A3. The scale is measuring the weight changes as the ice turns to water and drip down a pipe to the scales.

Figure A4. The bowl on the scales is filled, with molten water.

Figure A5. Measurement tools, transmitters for the scales and the temperature.

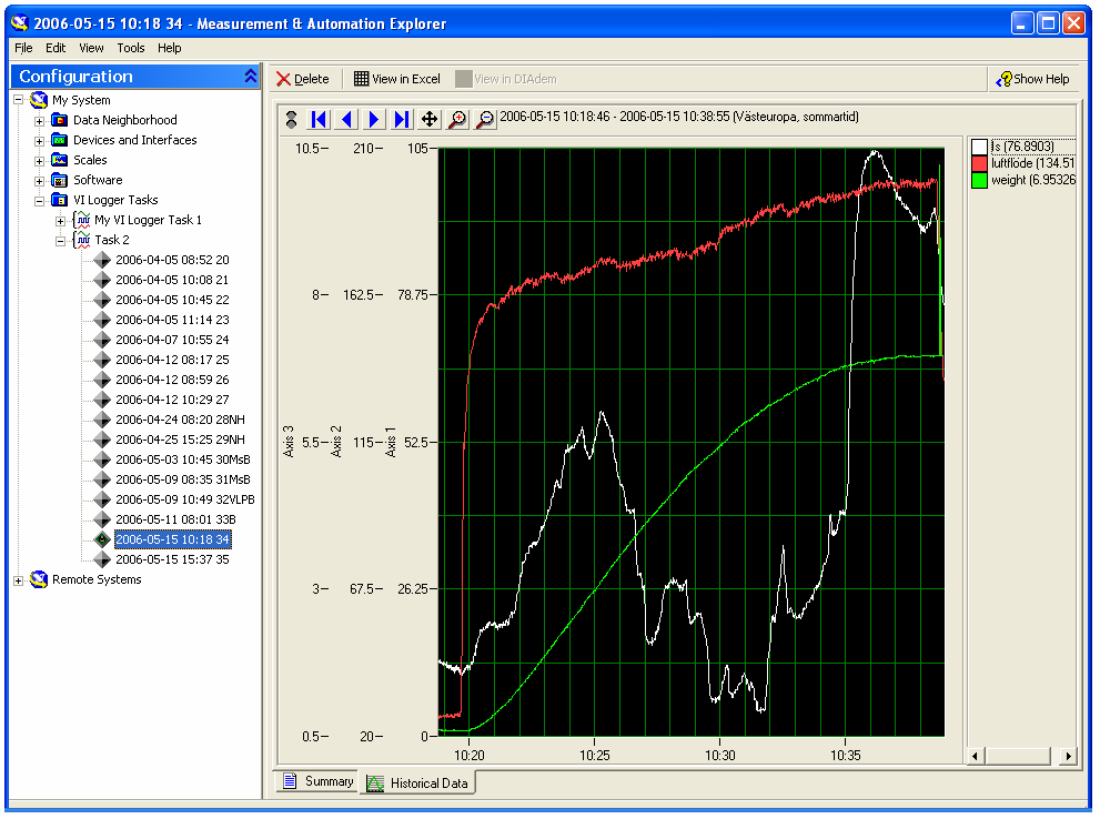

Figure A6. The Temperature of the ice and the airflow and the weight of the molten water are measured, and give files to compare and use.

Appendix 4

Tridiagonal matrix algorithm (TDMA)

The tridiagonal matrix algorithm (TDMA), also known as the Thomas algorithm, is a simplified form of Gaussian elimination that can be used to solve tridiagonal systems of equations. A tridiagonal system may be written as [30-31];

$$a_i x_{i-1} + b_i x_i + c_i x_{i+1} = d_i, \tag{A1}$$

where $a_1 = 0$ and $c_n = 0$. In matrix form, this system is written as

$$\begin{bmatrix} b_1 & c_1 & & & 0 \\ a_2 & b_2 & c_2 & & \\ & a_3 & b_3 & . & \\ & & . & . & c_{n-1} \\ 0 & & & a_n & b_n \end{bmatrix} \begin{bmatrix} x_1 \\ x_2 \\ . \\ . \\ x_n \end{bmatrix} = \begin{bmatrix} d_1 \\ d_2 \\ . \\ . \\ d_n \end{bmatrix}. \tag{A2}$$

For such systems, the solution can be obtained in $O(n)$ operations instead of $O(n^3)$ required by Gaussian Elimination. A first sweep eliminates the a_i's, and then a backward substitution produces the solutions. These types of matrices commonly arise from the discretization of 1D problems.

Fourier Biot

Conduction is described by the Fourier Biot law [31]:

$$q = -kA\nabla T \tag{A3}$$

where:
q – heat flow vector
k – thermal conductivity, a thermodynamic property of the material
A – a cross sectional area in direction of heat flow
∇T – Gradient of temperature (K/m)

$\nabla T = \left(\frac{\partial T}{\partial x}, \frac{\partial T}{\partial y}, \frac{\partial T}{\partial z} \right)$, in cartesian coordinates

$$\nabla T = \left(\frac{\partial T}{\partial r}, \frac{1}{r}\frac{\partial T}{\partial \theta}, \frac{\partial T}{\partial z} \right), \text{ in cylindrical coordinates}$$

Divengence Theorem

The divergence theorem, also called Gauss' theorem, Ostrograndsky's theorem, or Ostrogradsky-Gauss theorem is a result that relates the ourware flow oa a vecor field on a surface to the behaviour of the vector field inside the surface [31]. The theorem states that the flux of a vector field on a surface is equal to the triple integral of the divergence on the region inside the surface. Intuitively, it states that the sum of all sources minus the sum of all sinks gives the net flow out of a region. The divergence theorem is an important result for the mathematics of physics, in particular in electrostatics and fluid dynamics [31-32]. S = ∂V closed surface [32];

$$\iiint_V \left(\nabla \cdot \vec{\mathrm{F}}\right) dV = \oiint_S \vec{\mathrm{F}} \cdot \hat{n} dS \qquad \text{(A4)}$$

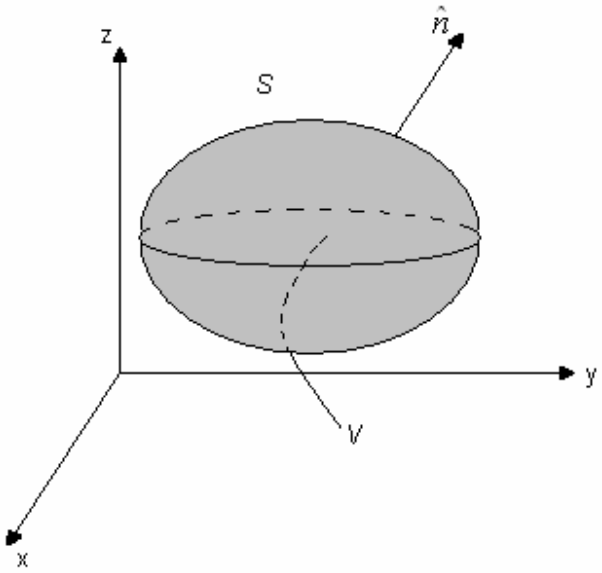

Figure A7. Volume, surface and unit vector.

Delaunay triangulation

I mathematics, and computational geometry, the Delaunay triangulation or Delone triangularization for a set **P** of points in the plane is the triangulation DT(**P**) of **P** such that no point in **P** is inside the circumcircle of any triangle in DT(**P**). Delaunay triangulations maximize the minimum angle of all the angles of the triangles in the triangulation; they tent to avoid "sliver" triangles. The triangulation was invented by Boris Delaunay in 1934 [31].

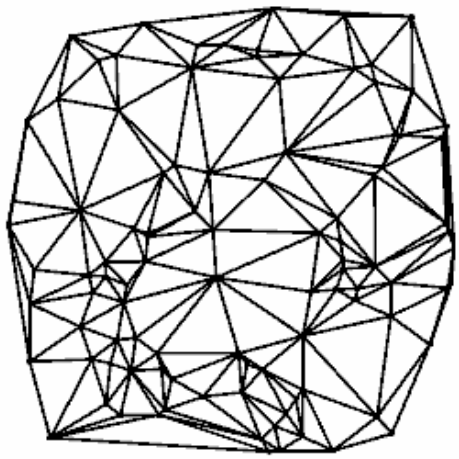

Figure A8. This is the Delaunay triangulation of a random set of points in the plane [31].

In the general n-dimensional case it is stated as follows: For a set **P** or points in the n-dimensional Euclidean space, the Delaunay triangulation is the triangulation DT(**P**) of **P** such that no point in P is inside the circum-hypersphere of any simplex in DT(**P**) [31].

It is known that the Delaunay triangulation exists and is unique for **P**, if **P** is a set of points in general position, that is, no three points are on the same line and no four are on the same circle, for a two dimensional set of points, or no $n + 1$ points are on the same hyperplane and no $n + 2$ points are on the same hypersphere, for an n-dimensional set of points [31].

This is easily seen that for the set of three points on the same line there is no Delaunay triangulation, in fact there is no triangulation at all. On the other hand, for four points on the same circle, e.g. the vertices of a rectangle, the Delaunay triangulation is not unique, clearly, the two possible triangulations that split the quadrangle into two triangles satisfy the Delaunay condition [31].

Generalizations are possible to metrics other than Euclidean. However in these cases the Delaunay triangulation is not guaranteed to exist or be unique.

Taylor series

Taylor's formula

$$f(x) = f(a) + \frac{f'(a)}{1!}(x-a) + \frac{f''(a)}{2!}(x-a)^2 + \ldots + \frac{f^{(n)}(a)}{3!}(x-a)^n + R_{n+1}(x) \qquad \text{(A5)}$$

, where

$$R_{n+1}(x) = \int_x^a \frac{(x-t)^n}{n!} f^{(n+1)}(t)dt = \frac{f^{(n+1)}(\xi)}{(n+1)!}(x+a)^{n+1} \qquad \text{(A6)}$$

where $\xi \in [a,x]$ [32].

Taylor series

If $R_n(x) \to 0$ as $n \to \infty$ then [32]

$$f(x) = \sum_{k=0}^{\infty} \frac{f^{(k)}(a)}{k!}(x-a)^k . \qquad \text{(A7)}$$

Weighted mean

Statistics has given a set of data, $X = \{x_1, x_2, ..., x_n\}$ and corresponding weights, $W = \{w_1, w_2, ..., w_n\}$, the weighted mean, or weighted average, is calculated as:

$$\bar{x} = \frac{\sum_{i=1}^{n} w_i x_i}{\sum_{i=1}^{n} w_i} \qquad \text{(A8)}$$

If all the weights are equal, the weighted mean is the same as the arithmetic mean. While weighted means generally behave in a similar fashion to arithmetic means, they do have a few counter-intuitive properties, as captured for instance in Simpson's paradox. Weighted

versions of other means can also be calculated. Examples of such weighted means include the weighted geometric mean and the weighted harmonic mean [31].

Permutation

A permutation is a bijection from a finite set *X* onto itself. A function *f* form a set *X* to a set *Y* is said to be bijective if and only if for every *y* in *Y* there is exactly one *x* in *X* such that *f*(*x*) = *y*. that is f is bijective if and only if it is a one-to-one correspondence between those sets, i.e. both one-to-one and onto. A bijective function is also called a bijection or permutation [31].

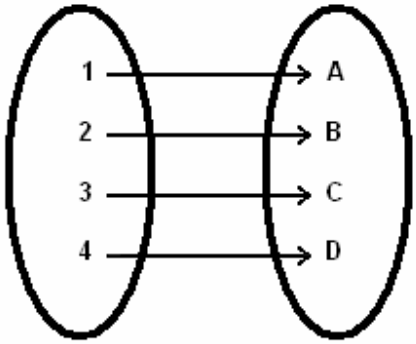

Figure A9. A bijective function.

Weak formulation

In general, the weak formulation of an equation is obtained by multiplying the partial differential equation by an appropriate smooth test function, i.e. taking into account the boundary equations, and integrating. This means that the equation is not required to hold absolutely, but has to hold for certain test functions [31].

R^2

In statistics, the coefficient of determination R^2 is the proportion of a sample variance of a response variable that is explained by the predictor variables when a linear regression is done. From [30];

$$R^2 = \frac{ESS}{TSS} = 1 - \frac{RSS}{TSS}$$

where *ESS* is the explained sum of squares, *RSS* is the residual sum of squares, and *TSS* is the total sum or squares. Total sum of squares is the explained sum of squares and the residual sum of squares. i.e.;

$TSS = ESS + RSS$

ESS is the sum of squared predicted values in a standard regression model;

$$y_i = a + bx_i + \varepsilon_i \quad \text{(A9)}$$

where y_i is the response variable, x_i is the explanatory variable, a and b are coefficients, i indexes the observations from 1 to n, and ε_i is the error term.

If $\hat{a}$ and $\hat{b}$ are the estimated coefficients, then

$$\hat{y}_i = \hat{a} + \hat{b}x_i \quad \text{(A10)}$$

is the predicted variable. The *ESS* is the sum of the squares of the differences of the predicted values and the grand mean:

$$\sum_{i=1}^{n} (\hat{y}_i - \bar{y})^2$$

RSS is the sum of squares of residuals. In a regression model like the one in Eq. (AR1), where a and b are coefficients, y and x are the regressand and the regressor, respectively, and ε_i is the error term. The sum of squares of residuals is the sum of squares of estimates of ε_i. Don't confuse error and residual. Error is the amount by which an observation differs from its expected value. Residual, on the other hand, is an observable estimate of the unobservable error. In case where there is just one scalar-valued predictor variable, R^2 is the square of the correlation between the predictor and response variables. R^2 will always increase when a new term is added to a model, unless the new term is perfectly multicollinear with the original terms. Adding a new term will never decrease R^2 [31].

It is important to know that R^2, does not tell whether:

- An included independent variable is statistically significant
- The independent variables are a true cause of the changes in the dependent variable
- Omitted-variable bias exists;
- The most appropriate set of independent variables have been chosen